THE ASTROPHYSICAL JOURNAL, 391:667–684, 1992 June 1

MODELING THE STELLAR CONTRIBUTION TO THE GALACTIC COMPONENT OF THE DIFFUSE SOFT X-RAY BACKGROUND. I. BACKGROUND FLUXES AND NUMBER COUNTS

V. KASHYAP
Department of Astronomy and Astrophysics, The University of Chicago, 5640 South Ellis Avenue, Chicago, IL 60637

R. ROSNER
Department of Astronomy and Astrophysics and Enrico Fermi Institute, The University of Chicago, 5640 South Ellis Avenue, Chicago, IL 60637

G. MICELA, S. SCIORTINO, AND G. S. VAIANA
Osservatorio Astronomico di Palermo, Palazzo dei Normanni, 90134 Palermo, Italy

AND

F. R. HARNDEN, JR.
Harvard-Smithsonian Center for Astrophysics, 60 Garden Street, Cambridge, MA 02138
Received 1991 January 21; accepted 1991 October 15

ABSTRACT

We estimate the contribution to the diffuse soft X-ray background flux from main-sequence A, F, G, K, and M stars, and RS CVn stars, at various energies ranging from 0.1 to ~ 5 keV, using a combination of a stellar Galaxy model based on optical data, stellar X-ray luminosity functions derived from the full *Einstein* data base, and a model for X-ray absorption derived from observed hydrogen column densities. We resolve previous discrepancies between earlier estimates of the stellar contribution to the diffuse soft X-ray background and find that this stellar contribution at high Galactic latitudes is less than 3% for photon energies less than 0.3 keV, 3%–17% in the medium-energy M1 and M2 bands (~ 0.4 to ~ 0.9 keV), and 10%–30% in the higher energy I and J bands (~ 0.8–2 keV), at a threshold sensitivity for point source detection $\sim 10^{-10}$ ergs s^{-1} cm^{-2}. At low latitudes, where the estimations are subject to large uncertainties, we estimate a stellar contribution of $<3\%$ below 0.3 keV, 7%–40% in the medium-energy bands, and 27%–70% in the I and J bands. We calculate the change in the magnitude of the diffuse flux arising from stellar emission when this threshold sensitivity is increased and find that the diffuse flux decreases only by a factor of 2 as this sensitivity is increased to $\sim 10^{-14}$ ergs s^{-1} cm^{-2}, and stars that were previously undetected become detections. We show that while dM stars are the major contributors to the diffuse stellar flux, other stellar types contribute as much as 40% of this flux at the higher energies in the passband studied. We show directly that line emission can be used as a diagnostic tool for constraining models of the background emission and explicitly demonstrate the sensitivity of diffuse flux estimates to the characteristics of the adopted models for the emission. Finally, we also find that our calculated log (N)–log (S) curves are consistent with the observed number of detections in the various *Einstein surveys.*

Subject headings: Galaxy: stellar content — X-rays: stars

1. INTRODUCTION

Extensive observations in the soft X-ray regime ≈ 0.1 to ≈ 4.5 keV since 1962 have demonstrated the existence of diffuse emission, with the portion above roughly 2 keV generally attributed in large part to extragalactic sources (see Schwartz & Gursky 1973). Observations below 2 keV, however, demonstrated that the flux in this regime was significantly enhanced above that expected even from extrapolation of unabsorbed extragalactic emission, and hence implied the presence of a nite Galactic component to the diffuse soft-X-ray background (see review by McCammon & Sanders 1990).

Is this Galactic component truly diffuse, or is it due to the unresolved contribution from discrete sources? Gorenstein & Tucker (1972) presented a model involving a discrete source distribution with a scale height of 800 pc and a luminosity of 3×10^{30} ergs s^{-1} in the soft energy 0.16–0.28 keV bandpass, based on the ratio of intensities at 0.16 and 0.28 keV. Later, Davidson et al. (1972) pointed out that the latitude dependence predicted by such a model is inconsistent with observations made at higher energies. They therefore proposed a simple two-component model, consisting of the superposition of an extragalactic and a Galactic component. However, as more detailed observations became available, this model too proved to be insufficiently complicated to account for the overall brightness distribution of the soft-X-ray background (cf. Tanaka & Bleeker 1977).

In order to permit further refinements in the models, it became clear that it was essential to establish the extragalactic contribution to the diffuse flux at low photon energies. An upper limit of 25% was placed on the fraction of extragalactic flux in the soft X-ray background around 0.25 keV by McCammon et al. (1971) who looked for the absorption of this component by the gas in the Small Magellanic Cloud. These authors showed that the data were inconsistent with standard absorption models (i.e., models based on absorption due to the Galaxy and the SMC, the Galaxy alone, and the SMC alone) unless only the extragalactic power-law hard background was absorbed. This limit was further reduced to 9% in the 0.1–0.28 keV band by Long, Agrawal, & Garmire (1976), who per-

formed a similar analysis on the soft-X-ray flux from the direction of the Large Magellanic Cloud. McCammon et al. (1976) reestimated this same fraction using more detailed 21 cm hydrogen column density data and obtained a 15%–22% contribution to the flux due to the extragalactic component (at the 2 σ level), and a 4%–5% contribution as the best-fit value. Thus, it appeared that while the diffuse X-ray background at high energies (>2 keV) was mainly extragalactic in origin, the diffuse background at the soft and medium energies (0.1–2 keV) must mainly be Galactic in origin. In addition, the main type of source contributing at the soft energies (<0.3 keV) must be different from the type of source that contributes at higher energies ($\sim$1 keV). The challenge then is to fix the natures of these contributors of this remaining, presumably Galactic, diffuse emission.

These arguments were demonstrated by Burrows et al. (1981; see also McCammon et al. 1983), who presented a three-component model for the total background, consisting of an absorbed extragalactic component, stellar coronal emission, and supernova cavities, with most of the contribution from the local cavity being in the low-energy C band. They argued that they could fit the data with a Raymond-Smith collisional equilibrium thermal spectrum (Raymond & Smith 1977) for solar abundances at a temperature of $\approx 10^6$ K and a best-fit ratio of 0.38 ($\pm$0.01) of the 0.1–0.18 keV and 0.15–0.28 keV bands and concluded that in these bands, the flux was due almost entirely to the emission from a local supernova remnant cavity. This conclusion was supported by measurements of the positional correlation of Galactic hydrogen and the soft X-ray flux by McCammon et al. (1983). These latter authors concluded that at energies greater than 2 keV, most of the flux must be extragalactic in origin; that in the range 0.5–1 keV, a Galactic component, in addition to the absorbed extragalactic component, is required; and, finally, that at energies less than $\sim$0.3 keV, the flux was anticorrelated with the observed hydrogen column density, but that the scatter was too large to be explained simply as a reflection of absorption of extragalactic flux. This lattermost point indicated the existence of a highly local component.

In this paper, we focus on the diffuse X-ray flux arising from local (i.e., Galactic) sources, and in particular reconsider the role played by discrete source emission due to ordinary Galactic stars. Stars have been known to be quasi-steady emitters in soft X-rays since the late 1970s (see review by Rosner, Golub, & Vaiana 1985), but previous to the flight of the *Einstein Observatory*, their contribution was considered insignificant because the luminosity and number density requirements set by Gorenstein & Tucker (1972) and Levine et al. (1977) seemed to exclude them. For example, the required soft X-ray luminosity of stars was shown to be greater than the observed luminosities of 50 nearby stars in a survey carried out as part of the *Skylab* program by Vanderhill et al. (1975), which led them to conclude that emission from stars was unlikely to contribute significantly to the diffuse Galactic background at energies below 0.3 keV. Similarly, Levine et al. (1977) derived a required lower limit of 0.2 pc^{-3} for the average number density of sources at 0.13 keV, using the observed fluctuations in the intensity of X-rays of $\approx$9% per 0.01 sr beamwidth; this number density is of course greater than the local density of all known types of normal stars, and hence this argument also pointed against a significant contribution from normal stars. Thus, normal stars could not be the major contributor to the diffuse background at soft energies.

TABLE 1

PASSBAND DEFINITIONS

Bandwidth (keV)	Name
0.078–0.11	Be
0.10 –0.18	B
0.15 –0.28	C
0.10 –0.28	L
0.28 –1.00	M0
0.45 –0.65	M1
0.65 –0.85	M2
0.45 –0.85	M
0.85 –1.15	I
1.15 –2.00	J
0.15 –4.00	E[a]
0.10 –2.40	R[b]

[a] The full *Einstein band*, as used in this paper.
[b] The full *ROSAT* band.

The first estimate of the stellar contribution to the background (Rosner et al. 1981), based on actual detections of soft X-ray emission from ordinary solar-like stars, suggested a contribution to the Galactic diffuse background ranging from $\approx$6% to 24% in the medium-energy M0 band (see Table 1); this estimate was obtained by assuming an exponential density distribution of stars perpendicular to the Galactic disk, stellar density values and scale heights given by Allen (1973), and mean stellar X-ray luminosities based on the early *Einstein Observatory* results. Rosner et al. (1981) used an analytical expression for the diffuse X-ray flux received from a given direction,

$$f_{\rm star}(b) = \frac{1}{4\pi} \sum_i n_i(0) \langle L_x \rangle_i H_i \text{ ergs s}^{-1} \text{ cm}^{-2} \text{ sr}^{-1}, \quad \text{(1a)}$$

where

$$n_i(r) = n_i(0) \exp\left(-\frac{r \sin(b)}{h_i} - \frac{r}{l}\right) = n_i(0) \exp\left(-\frac{r}{H_i}\right) \quad \text{(1b)}$$

is the space density of a given star type i at a distance r, $n_i(0)$ is the corresponding space density in the Galactic equatorial plane, b is the Galactic latitude, h_i is the actual scale height of the star type being considered, l is the effective photon mean free path in the interstellar medium, H_i is the corresponding effective stellar scale height (defined as above), and $\langle L_x \rangle_i$ is the mean X-ray luminosity of a given stellar type; they estimated the flux in the 0.28–1.0 keV band to be

$$f_{\rm star}(0.28\text{–}1.0 \text{ keV}; b = 90°) = 2.5(+1.1, -0.8) \times 10^{-9} \text{ ergs cm}^{-2} \text{ s}^{-1} \text{ sr}^{-1},$$

compared to the total X-ray background flux (from Fried et al. 1980) of

$$f_{\rm total}(0.28\text{–}1.0 \text{ keV}) = (1.5\text{–}3.1) \times 10^{-8} \text{ ergs cm}^{-2} \text{ s}^{-1} \text{ sr}^{-1},$$

leading to the conclusion that $\approx$11%–24% of the minimum and $\approx$6%–12% of the maximum observed diffuse background X-ray flux can be accounted for by stellar coronal X-ray emission. The photon mean free path was taken to be 200 pc.[1] The

[1] This approximation is rather severe, since the mean free path can change from $\sim$10 to $<10^3$ pc over this energy range. For this reason, we shall use hydrogen column densities, coupled with X-ray absorption cross sections for the interstellar medium, while calculating optical depths.

TABLE 2

MEAN X-RAY LUMINOSITIES (AND 68% CONFIDENCE LIMITS), SCALE HEIGHTS, AND DENSITY OF DIFFERENT STELLAR TYPES IN THE SOLAR NEIGHBORHOOD

Star Type	Scale Height (pc)	$n(0)$ (pc^{-3})	log $\langle L(\text{ergs s}^{-1})\rangle$
A/F[a]	190	0.003	29.0
A	70	0.0005	28.31 (+0.24, −0.57)
F	180	0.0025	28.87 (+0.06, −0.07)
G[a]	340	0.006	27.8
G	340	0.006	28.43 (+0.10, −0.12)
K[a]	350	0.01	27.8
K	350	0.01	28.54 (+0.12, −0.15)
M[a]	350	0.065	28.36 (±0.17)
M[b]	...	0.065	28.36 (+0.19, −0.41)
M[c]	350	...	28.18
M(Blue)	350	0.025	28.62 (+0.16, −0.23)
M(Red)	350	0.040	27.87 (+0.20, −0.37)
RS CVn	110	0.0001	30.65 (+0.15, −0.21)

NOTE.—Scale heights and $n(0)$ values are from Rosner et al. 1981 for G and K stars; from Bahcall & Soneira 1980 and Allen 1973 for A, F, M(Blue), and M(Red) stars; and from Hall 1976, for RS CVn stars. Favata et al. 1988 and Favata 1987 used Hall's (1976) estimate of the space density, $n(0)$, for eclipsing systems, and estimates of stellar dimensions and orbit sizes, in order to compute an approximate space density for the entire class of RS CVn objects regardless of whether they are eclipsing or not.

[a] As used by Rosner et al. 1981.

[b] As used by Caillault et al. 1986.

[c] As used by Schmitt & Snowden 1990.

A and F stars were combined into a single set, and the values adopted for the remaining variables are listed in Table 2.

One important point is the large statistical uncertainty of these results. This uncertainty comes about because the mean stellar luminosity is primarily fixed by the high-luminosity tail of the stellar X-ray luminosity function, and in the survey data used, this tail is highly uncertain. Caillault et al. (1986) recognized this difficulty and used a different approach to estimate the tail contribution: They used an X-ray–selected, flux-limited sample to construct an M star luminosity function that better represents the high-luminosity tail which contributed most of the flux in Rosner et al. (1981) and calculated the fraction of M dwarfs with luminosities greater than or equal to a limiting threshold by taking the ratio of the surface density of detected M dwarfs with luminosities higher than the threshold within a limiting distance, to the total surface density of M dwarfs within that distance. By then comparing this number to the number predicted by the X-ray luminosity function used by Rosner et al., Caillault et al. (1986) found that their flux-limited, X-ray–selected sample of high-luminosity stars contributed $<8\%$ to the soft X-ray background in the 0.28–1.0 keV band, a factor of 2 lower than that predicted by Rosner et al. Thus, they conclude, stars contribute less than 10% of the background flux in the 1 keV range.

However, Caillault et al. (1986) neglected to take into account both the variation of stellar density with height above the Galactic disk and absorption in the ISM, thus overestimating the number of M dwarfs in the region of interest. Therefore, the fractions of M dwarfs with luminosities greater than or equal to a threshold luminosity, as calculated by them, would be smaller than in reality, and consequently, the flux predicted by using the mean luminosity computed from their luminosity function would be less than that estimated by Rosner et al. (1981). For example, a mean X-ray luminosity of $\sim 10^{28}$ ergs s^{-1} was calculated from the luminosity function which assigned all dM stars with unknown spectral type to M0, which is less than the mean luminosity of 2.3×10^{28} ergs s^{-1} used by Rosner et al., and also less than the mean luminosity of 4.3×10^{28} ergs s^{-1} calculated from the luminosity function for early M stars (Bookbinder 1987, see § 2) with $B-V < 1.63$.

Caillault (1990) extended and improved the luminosity function constructed by Caillault et al. (1986) by using better estimates for visual magnitudes and extending the survey to include M dwarfs detected in the *Einstein* Extended Medium Sensitivity Survey and arrived at the same conclusion as before, viz., that stars contribute less than 10% to the diffuse X-ray background at the 1 keV range. However, as before, the number of M dwarfs in the region of interest are overestimated, leading to an underestimate of their contribution.

Most recently, Schmitt & Snowden (1990) have refined estimates of the M dwarf contribution to the diffuse background by adopting a continuous emission measure distribution model for stellar coronal emission (in order to provide a physically more appropriate description of stellar coronal emission) and used it to compute the stellar X-ray contributions in various bands; as we do, Schmitt & Snowden used the galaxy model constructed by Bahcall & Soneira (1980). They find that M dwarfs contribute negligibly at energies below 0.3 keV and contribute up to 10% of the background around 1 keV at high latitudes. At low latitudes, they find a larger contribution, but those estimates are highly uncertain because of the uncertainties involved in estimating the interstellar absorption in the plane of the galaxy (see discussion in § 4.1). Schmitt & Snowden also seriously underestimate the high-luminosity tail of the M dwarf X-ray luminosity function, and the value they adopt for the mean X-ray luminosity, 1.5×10^{28} ergs s^{-1}, is less than the 68% lower confidence limit obtained for the early type M dwarfs (see § 3), leading to their low estimate of the stellar background contribution at high latitudes. Their underestimate of the mean luminosity is due to the difference between their adopted analytical lognormal form for the luminosity function, and the high-luminosity tail of the dM star X-ray luminosity function (see their Fig. 4).

In this paper we improve upon earlier work by calculating the soft X-ray flux emitted by all main-sequence stars at high Galactic latitudes over a wide range in energy, and also in some specific passbands (see Table 1 for passband conventions used here), using a plausible model for the stellar space distribution within our Galaxy, based on Bahcall & Soneira (1980) and Bahcall (1986), improved stellar X-ray luminosity functions derived from the full *Einstein* stellar data base (Micela et al. 1991), and measured values for the hydrogen column density where available (our calculations show the consequences of either adopting the Heiles & Habing 1974 measurement, or the mean model of Bloemen 1987). As we shall show, high spectral resolution background measurements in the soft X-ray band turn out to be very sensitive to the details of the models for the background, far more than either broad-band (e.g., filter) measurements at these same energies, or high-resolution measurements at higher energies. We estimate the background flux and the number of stars detected as a function of the threshold point source sensitivities by taking into account the fact that stellar contribution to the diffuse background decreases as point source sensitivity is increased (and the number of stars detected as point sources therefore increases). We construct log (N)–log (S) curves and examine

the effects of varying the parameters of the model describing stellar coronal emission. A description of the data used, including the X-ray luminosity functions used in this paper, is presented in § 2. The modeling process, involving the calculation of the background fluxes, the log (N)–log (S) curves and corresponding confidence limits, is discussed in § 3. Results of the calculations are presented in § 4; and § 5 summarizes our results.

2. THE DATA

All X-ray luminosity functions used here except that for RS CVn stars make use of censored data (i.e., data contain upper limits as well as detections) and are constructed using survival analysis methods as set out by Schmitt (1985) and Feigelson & Nelson (1985).

The A star X-ray luminosity function, containing 16 stars with four detections, was constructed using all stars within 30 pc among those listed by Schmitt et al. (1985) by considering all main-sequence X-ray emitters with $0.1 < B-V < 0.3$; the luminosities are in the 0.15–4.0 keV band. The F star luminosity function, with 32 detections and 10 upper limits, is from the same source: All stars with $0.3 < B-V < 0.5$ and within 30 pc among those listed by Schmitt et al. (1985) were used. The main-sequence G star luminosity function with 32 detections and 29 upper limits for all *Einstein* IPC (Imaging Proportional Counter) observed stars of the luminosity classes IV and V in the spectral range F7–G9, located within 25 pc, was constructed by Maggio et al. (1987). The main-sequence K star luminosity function, with 43 detections and 33 upper limits, was constructed using the luminosity function for K stars within 25 pc constructed by Bookbinder (1987), but updated to correspond to the full *Einstein* data set now available (cf. Micela et al. 1991). The luminosity function for M stars within 10 pc given in the same source (Bookbinder 1987) was split into two sets—Blue stars, with $B-V < 1.65$ and Red stars, with $B-V > 1.65$—and further revised to form the M(Blue) (28 detections, 16 upper limits) and M(Red) (22 detections, three upper limits) luminosity functions. The luminosities are for the 0.1–3.5 keV band. The RS CVn luminosity function (nine detections) is based on the data presented in Majer et al. (1986). All detected RS CVn stars within 35 pc were used to construct the X-ray luminosity function. Favata et al. (1988) used the same data set of Majer et al. (1986) in their analysis of excess yellow dwarfs in the *Einstein* Medium Sensitivity Survey but considered all (RS CVn) stars within 100 pc; our aim is to construct a less biased sample for the high-luminosity tail of the luminosity function, based on the truncated set of RS CVn stars we are using. These luminosity functions are plotted in Figure 1, along with their means and the 68%, 95%, and 99% confidence limits on the means. The confidence limits were obtained by bootstrapping the luminosity functions as follows: Using a random number generator taken from Press et al. (1986), we generate a bootstrap luminosity function by sampling from the original luminosity function. This randomly generated luminosity function has the same number of stars as the original luminosity function. This procedure is carried out 10,000 times, and a mean luminosity is calculated each time. The resulting distribution of the means provide the confidence level intervals on the maximum likelihood value of the mean.

To account for interstellar absorption of X-rays, we use the hydrogen column densities calculated from the 21 cm data of Heiles & Habing (1974) at high Galactic latitudes ($|b| > 20°$), the three-component model of Bloemen (1987) describing the mean distribution of H I gas in our Galaxy, and the empirical relation at low latitudes ($|b| < 20°$) quantifying the hydrogen column density in the plane of the Galaxy (Dickey & Lockman 1989). Wherever we present calculations toward a specific direction (e.g., the north Galactic pole), we use the measured or the empirically determined column density to normalize the Bloemen model to this column density as described in § 3.5. In other cases, we use the column densities as predicted by the average model. In order to calculate the attenuation at a given photon energy, and a given H I column density, we have adopted the piecewise polynomial fit to the interstellar photoelectric absorption cross sections in the 0.03–10 keV range as determined by Morrison & McCammon (1983). This fit has been modified to account for the presence of molecular hydrogen close to the Galactic plane, based on the data presented in Cruddace et al. (1974). The correction for the presence of molecular hydrogen at an energy ϵ keV,

$$\sigma_{H_2} = 0.16 \times 10^{-22} f_{H_2} \epsilon^{-3.54} \quad (\epsilon \geq 0.0124 \text{ keV}), \qquad (2)$$

where f_{H_2} is the ratio of the column density of H_2 to that of H I, as determined from a model describing the average properties of the ISM (Bloemen 1987; see § 3.5).

3. THE CALCULATIONS

Our model calculations combine stellar X-ray spectra based on a thermal plasma spectrum (Raymond & Smith 1977; Raymond 1986) with the galaxy model of Bahcall & Soneira (1980; also Bahcall 1986) and use the observed stellar X-ray luminosity functions. To account for absorption, we adopt a three-component description of the interstellar medium (from Bloemen 1987) and normalize it to the measured total hydrogen column densities (from Heiles & Habing 1974). The basic idea is to calculate the flux from a star of a given spectral type in a given band, and then to calculate the attenuated total flux in a given direction using the stellar number counts generated by the galaxy model. The thermal spectrum is calculated at a given temperature, for given abundances, taking into account both line and continuum emission.

3.1. *The Galaxy Model*

The galaxy model of Bahcall & Soneira (1980) is a two-component model of the Galaxy, containing an exponential disk and a de Vaucouleurs spheroid component (which has a light distribution similar to that of an elliptical galaxy). It is designed to provide the expected main-sequence dwarf and giant star counts within a specified solid angle as a function of latitude, longitude, and absolute visual magnitude. Stellar optical luminosity functions and scale heights are derived from local observations, and the assumed global forms of the density laws are derived from accurate measurements of the light distributions in other galaxies. The model apparently accurately reproduces the density variations for all longitudes, and for latitudes $>20°$. The data from Luyten (1968) and Wielen (1974) are fitted to an analytic function. Both the disk and the spheroid have the same stellar optical luminosity function over the range of magnitudes that contributes most to the counts. In this paper, we assume that spheroid and disk stars of the same spectral type have the same X-ray luminosity functions.[2] The

[2] This assumption is most likely invalid, but the very sparse X-ray data available for spheroid stars prevent a more appropriate description. However, since the spheroid component is not a major contributor to the diffuse background (see Fig. 7), our assumption is not critical.

scale heights of the stars are also a function of magnitude and vary from 90 to 325 pc.

3.2. *The Stellar X-Ray Spectrum*

A crucial difference between the diffuse X-ray background at soft X-ray energies (<4 keV) and the corresponding background at higher energies is that because many of the dominant contributors at soft X-ray energies are thermal sources, their spectra are completely dominated by lines. As a consequence, monochromatic diffuse background measurements at soft X-ray energies are extremely sensitive to the details of the assumed models for the background sources—simple power-law index descriptions are entirely inappropriate at these energies. This complexity does, however, have its reward, namely that high spectral resolution background measurements can be very constraining for models of the background. In order to illustrate this situation, we have considered two distinct models for the stellar component of the background, both of which are designed to be consistent with available stellar spectral data obtained from the *Einstein* Imaging Proportional Counter (Schmitt et al. 1990), and have treated them by considering the resulting stellar background contribution both in broad bands and in high spectral resolution calculations.

The first type of model is based on the idea that stellar coronae are composed of two distinct types of "loop atmospheres," namely a hot active component and a somewhat cooler quiescent component (cf. Rosner et al. 1985). Thus, we assume stellar coronal emission to consist of two temperature components, with the active regions at a nominal temperature $T_a = 1.74 \times 10^7$ K and the quiet regions at a temperature $T_q = 1.4 \times 10^6$ K, both corresponding to the best-fit two-temperature models derived from observations (see Schmitt et al. 1990). We use the X-ray spectrum of Raymond (1986;

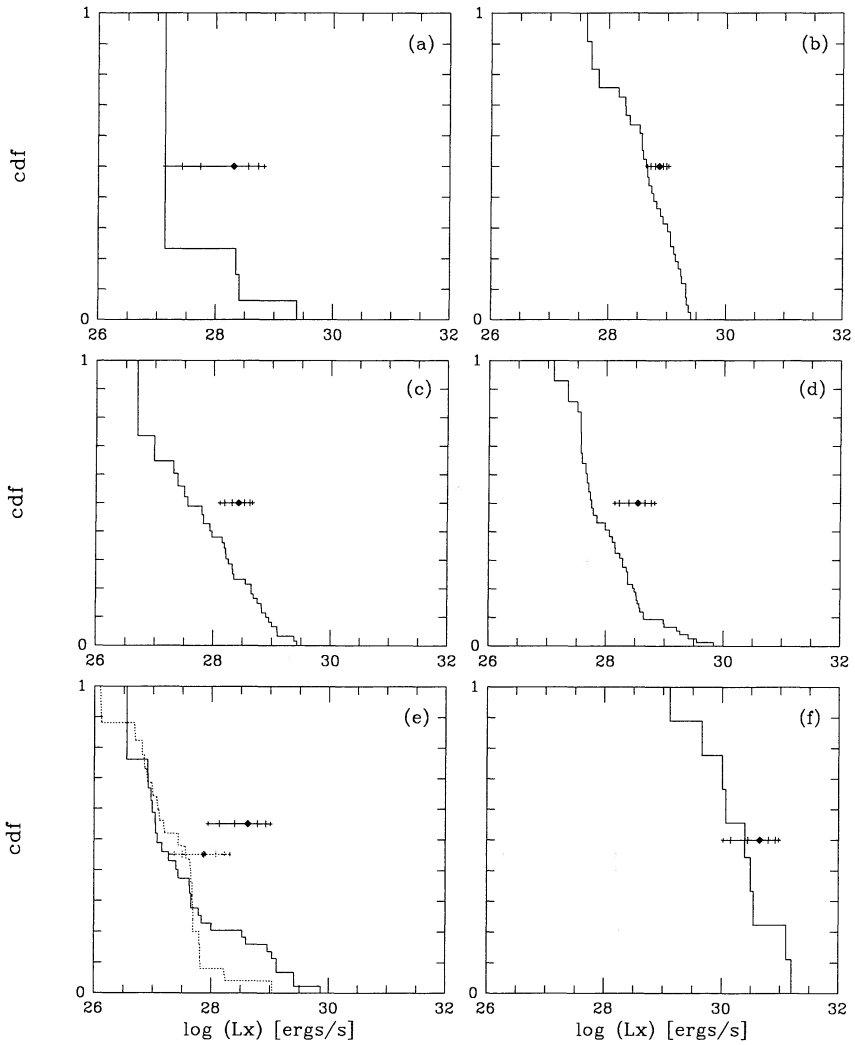

FIG. 1.—The integral X-ray luminosity functions. In each case, the ordinate represents the probability of a star having a soft X-ray luminosity greater than or equal to the X-ray luminosity given on the abscissa. The solid square is the mean luminosity for the sample; cross marks on either side give the 68%, 95%, and 99% confidence levels on this mean. (*a*) The A star luminosity function (from Schmitt et al. 1985). (*b*) The F star luminosity function (from Schmitt et al. 1985). (*c*) The G star luminosity function (Maggio et al. 1987). (*d*) The K star luminosity function (based on Bookbinder 1987). (*e*) The solid line is the M(Blue) ($B-V < 1.65$) star luminosity function (based on Bookbinder 1987). The dashed line is the M(Red) ($B-V > 1.65$) star luminosity function (based on Bookbinder 1987). The mean luminosity and confidence levels on this mean are connected by the same line type as the luminosity function. (*f*) The RS CVn star luminosity function (from Majer et al. 1986).

Raymond & Smith 1977) to construct the contributions in different passbands.[3]

The spectra for this model are determined as follows: First, the relative weights of the two components are determined by calculating the fraction of the surface of the star covered by active regions, $f_{\rm active}$. This is calculated by interpolating a given observed luminosity L_x between the extreme luminosities $L_{x,A}$ and $L_{x,Q}$

$$f_{\rm active} = \frac{L_x - L_{x,Q}}{L_{x,A} - L_{x,Q}}, \tag{3}$$

where $L_{x,A}$ is the luminosity that a star would be observed to have if it were covered entirely by active regions, and $L_{x,Q}$ is the luminosity that the star would be observed to have if it were covered entirely by structures similar to that observed on the Sun during its quiescent phase. These extreme luminosities are obtained by scaling the equivalent values obtained for the Sun (for the Sun, $L_{x,A}$ is 2×10^{29} ergs s^{-1}, and $L_{x,Q}$ is 5×10^{27} ergs s^{-1}; Vaiana & Rosner 1978) by a scale factor that takes into account the variations in the volume of the emitting plasma with stellar radius, plasma temperature, surface gravity, and the interception of flux by the stellar photosphere. This scaling is of the following form: The luminosity observed from an isothermal coronal plasma is

$$L_x(T) = 2\pi\epsilon(T)R^3 q(x), \tag{4}$$

where $\epsilon(T)$ is the energy emitted per unit volume of the plasma at a temperature T per unit time, R is the radius of the star,

$$q(x) = x + x^2 + (\tfrac{1}{3})x^3 + (\tfrac{1}{3})(2x + x^2)^{3/2} \tag{5}$$

is a "volume correction factor" that takes into account the interception of flux by the stellar photosphere, and

$$x = \frac{\pi k_B T}{2\mu m_{\rm H} g_* R} \tag{6}$$

is the scale height of emission at the temperature T on a star with surface gravity g_*, in units of the stellar radius, R. $L_{x,A}$ and $L_{x,Q}$ are obtained from the corresponding solar values by using this form of scaling. Note that in the limit of small x, i.e., small emission scale heights, this relation reduces to the familiar R^2 scaling of luminosities. Since the X-ray luminosity functions are binned into distinct spectral types, radii of 1.866, 1.2, 0.95, 0.74, 0.6, and 0.4 in units of the solar radius are used in the conversion for A, F, G, K, M(Blue), and M(Red) star types, respectively. No such scaling has been applied to RS CVn stars; instead, we adopt a fixed two-component spectrum (see Majer et al. 1986), with a high-temperature component ($T \sim 10^{7.2}$ K) contributing 83% of the emission and a low-temperature component ($T \sim 10^{6.4}$ K) contributing the rest, to describe the emission from all RS CVn stars. We adopt these values by averaging over the parameters given by two-temperature fits of various RS CVn systems obtained by Majer et al. (1986; see their Table 4).

The emission measure EM (defined so that $L_x = {\rm EM} \times P(T)$, where $P(T)$ is the power emitted by a unit volume of plasma at a temperature T for a single-temperature model) is normalized in all cases by calculating the power emitted by each of the two components, and by requiring that

$${\rm EM} = \frac{L_x}{f_{\rm active} P(T_a) + (1 - f_{\rm active}) P(T_q)}. \tag{7}$$

If L_x is greater than the luminosity assumed for the completely active star, it is assumed that the star is completely covered with active regions, and that the emission measure is large enough to account for the entire luminosity. A similar assumption is made if the luminosity considered is less than the luminosity assumed for the quiet star—the emission measure is assumed to be small enough to account for the entire luminosity as due to the quiet regions. Bandpass conversions are accomplished by using the spectra thus determined.

Computed background fluxes are relatively insensitive to variations in the temperature adopted for the quiet component but are quite sensitive to variations in the temperature adopted for the active component. The effects of adopting different values for these temperatures on model calculations are discussed further in § 3.6.

The second type of model attributes the observed X-ray emission as due to a continuous, power-law emission measure distribution, based on models describing observations of isolated solar coronal loops (see Schmitt et al. 1990). This emission measure distribution is of the form DEM $\sim T^{\alpha}$. Following Schmitt & Snowden (1990), we have adopted a maximum temperature $T_{\rm max} = 10^{7.1}$ K and the index of the power law, $\alpha = 0.9$. All spectral types are assumed to have the same spectrum except for RS CVn stars, where, as before, we use a fixed two-component "average" spectrum as being representative of all RS CVn stars. For a given luminosity L_x, this spectrum is normalized by requiring that the total emission measure must produce a source luminosity corresponding to L_x. Unless stated otherwise, we have used the two-temperature model in our calculations. The two models are compared in § 3.7.

3.3. *The Diffuse Flux*

Based on the star counts $n(r, l, b)$ pc^{-3} generated by the galaxy model, we compute the diffuse X-ray flux due to stars, f_x, via the integral

$$f_x(l, b) = \int dL\, dr\, d\Omega r^2 n(r, l, b) e^{-\tau(r)} \frac{L}{4\pi r^2} f(L) \tag{8a}$$

for each spectral type. Here $f(L)$ is the X-ray luminosity function for the given star type; $\tau(r)$ is the optical depth to distance r (this will be discussed in detail below); the typical solid angle Ω we consider is 1 deg^2. The lower limit for the r integration is set by the condition $r > r_{\rm min}$, where $r_{\rm min}$ is defined implicitly by

$$S = e^{-\tau(r_{\rm min})} \frac{L}{4\pi r_{\rm min}^2}, \tag{8b}$$

where S is the limiting sensitivity of the observing instrument. If the flux at Earth due to a star of luminosity L is less than the given sensitivity level, this flux is attributed to the background flux; if it exceeds the sensitivity threshold, the corresponding flux is attributed to detected sources. As the sensitivity is increased, the precise shape of the luminosity function becomes important to the diffuse flux determination as more stars become detected and cease to contribute to the diffuse background; for low sensitivities ($S > 10^{-12}$ ergs s^{-1} cm^{-2}), the shape of the luminosity function is essentially irrelevant to the diffuse background determination. Precisely the opposite is

[3] In general, we assumed that the measurements were made in the 0.15–4.0 keV band; the error made in taking the K and M star luminosity functions (measured in the 0.1–3.5 keV band) to be in this full *Einstein* band (0.15–4.0 keV) is negligible for coronal temperatures of interest.

true for the stellar number count determination: The exact shape of $f(L)$ is crucial to stellar number counts for low-sensitivity observations, but becomes less and less important as the sensitivity increases. We demonstrate this effect explicitly when we calculate log (f_{star})–log (S) curves (see below).

We calculate the change in the background flux as the threshold sensitivity of detection is increased as follows: For each value of the star counts generated by the galaxy model $n(r, l, b)$, we calculate the fraction of the stars whose X-ray flux at Earth would be of smaller magnitude than the given threshold sensitivity of detection, and hence would be unresolved. The flux due to these stars contributes to the diffuse background. This procedure is performed for various levels of sensitivities, and values for the background flux are obtained at each level, building up a log (f_{star})–log (S) curve. In other words, we perform the r-integration first in equation (8a).

Confidence limits on these curves are set by generating a total of 3000 distinct realizations of the log (f_{star})–log (S) curves, obtained in the following manner. First, a luminosity function for a given spectral type is generated as described in § 2. Then, at each radial distance step in the galaxy model, the number of stars $dn(r)$ predicted by it is obtained. Using an incomplete gamma function distribution (Press et al. 1986), we then define a sample of 30 distinct realizations of the stellar sample at each of these distance steps [the mean number of stars, averaged over all realizations, is $dn(r)$], and calculate a diffuse flux resulting from unresolved stars at each sensitivity level. Thus, we obtain 30 realizations of the log (f_{star})–log (S) curve for the given realization of the luminosity function. A total of 100 realizations of the luminosity function are used, resulting in a sample of 3000 log (f_{star})–log (S) curves. Confidence limits are then set on the calculated diffuse fluxes at each sensitivity level.

For low sensitivities, i.e., large values of S, the L integration can be performed first since the shape of the luminosity function $f(L)$ is irrelevant. Thus, the background flux is well approximated by

$$f_x(l, b) = \int dr\, d\Omega r^2 n(r, l, b) e^{-\tau(r)} \frac{\langle L_x \rangle}{4\pi r^2} , \quad (9)$$

where $\langle L_x \rangle$ is the mean luminosity of stars of the given spectral type. We use this method to estimate the background flux due to stars in all cases when point source sensitivity $S > 10^{-12}$ ergs s^{-1} cm^{-2}. The confidence level intervals obtained on the mean luminosities (as described in § 2) are used in the calculation of the background flux and provide a measure of the statistical uncertainties of the background flux due to the uncertainties in the luminosity functions.

3.4. *The Stellar* log N–log S

The stellar log ($N > S$)–log (S) curves were constructed as follows. The number of stars with a flux greater than a given sensitivity level, S, is given by

$$N(>S, l, b) = \int_0^\infty dL\, F(L) \int_0^{r'} r^2\, dr\, d\Omega n(r, l, b) , \quad (10a)$$

where r' is defined implicitly by the relation

$$S = \frac{L}{4\pi r'^2} e^{-\tau(r')} \text{ ergs s}^{-1} \text{ cm}^{-2} . \quad (10b)$$

If the stellar density were constant, if the X-ray luminosity function were a δ-function [i.e., $f(L) = \delta(L - \langle L \rangle)$], and if we neglected absorption, we would obtain the analytical expression

$$N(>S) = 0.094 n(0) \langle L \rangle^{3/2} S^{-3/2} ,$$

or

$$\log (N > S) = \text{constant} - \tfrac{3}{2} \log S . \quad (11)$$

This simple result must be modified by three effects: First, we must account for the actual distribution of stars in our Galaxy; second, we need to take the actual form of the stellar X-ray luminosities into account; third, we must include the attenuation of flux due to interstellar absorption. Thus, we adopt the above mentioned galaxy model; we use the X-ray luminosity functions discussed in § 2; and we use the absorption model discussed immediately following. The result cannot be expressed analytically but requires numerical integration of equation (10).

Confidence limits on the log N–log S curves are set in a manner similar to the method outlined in the previous section in the case of log (f_{star})–log (S) curves. A sample of 3000 log (N)–log (S) curves are obtained by bootstrapping the luminosity function and the galaxy model. The number of stars *detected* at each sensitivity step is computed for each sample, and confidence limits are then set on these detected stars at each sensitivity step.

3.5. *Absorption*

As mentioned above, X-ray absorption cannot be ignored. But while the absorption cross section (see § 2, eq. [2]) is reasonably well defined, the same cannot be said of the H I distribution in the Galaxy. Indeed, due to the complexity of the structure of the interstellar medium, a detailed accounting of the H I is not possible. We are therefore forced to adopt simplified models describing the average structure of the interstellar medium. Following Bloemen (1987), we adopt a three-component model describing the gas distribution in the Galaxy, involving the following:

1. A dense and cold ($T \approx 80$ K) component distributed as a Gaussian with a scale height $h_{cg} = 135$ pc and a midplane density $n_{cg} = 0.3$ cm^{-3}; and
2. A warm ($T \approx 8000$ K) medium surrounding the cold clouds, which has a nonuniform degree of ionization, and consists of a subcomponent distributed as a Gaussian with scale height $h_{wg} = 135$ pc and a midplane density $n_{wg} = 0.07$ cm^{-3}; and an exponentially distributed subcomponent with scale height $h_{we} = 400$ pc and a midplane density $n_{we} = 0.1$ cm^{-3}.

In addition to these two components, the molecular hydrogen is assumed to follow a Gaussian distribution, with a scale height of 70 pc and a midplane density of 0.3 cm^{-3}. At high latitudes,[4] $N(H_2)$ is $\approx 26\%$ of N(H I), and hence represents a meaningful correction to the opacity and therefore must be included in our absorption model (see § 2; eq. [2]). In summary, the number density of H I at a height z above the Galactic plane is

$$n_{H\,I}(z) = 0.3 e^{-(1/2)(z/h_{cg})^2} + 0.07 e^{-(1/2)(z/h_{wg})^2} + 0.1 e^{-(z/h_{we})} \text{ cm}^{-3} . \quad (12a)$$

[4] We confine our attention to high Galactic latitudes, with two exceptions (see Table 3 and Fig. 6) for two reasons: First, the optical galaxy model has not been tested for latitudes $|b| < 20°$; second, there is no reliable way to account for errors introduced by the patchiness of the absorption, and the increased attenuation of the X-ray flux due to molecular absorption in the plane of the Galaxy.

However, as pointed out above, the structure of the interstellar medium is very complex, and though the above model describes the gas distribution accurately on average, at specific pointings the measured H I column density (viz., Heiles & Habing 1974) differs significantly from that predicted by this model (e.g., toward the north Galactic pole, the measured column density is 0.66 of the predicted value, and for $b = 55°$, the measured column densities at $l = 170°$, 0°, and 250° are 0.16, 0.94, and 2.87 of the predicted column density, respectively). Therefore where necessary, we normalize the above model for each direction to the measured hydrogen column density to infinity in that direction. For latitudes $|b| > 20°$, we adopt the column density as measured by Heiles & Habing (1974) from 21 cm observations, and for latitudes $|b| \leq 20°$, where high opacities cause 21 cm measurements to underestimate the actual amount of hydrogen along the line of sight, we use the empirical relation for the hydrogen column density given by Dickey & Lockman (1989),

$$N_H = [3.84 \csc(|b|) - 2.11] \times 10^{20} \text{ cm}^{-2} . \quad (12b)$$

Specifically, we fix the scale heights of the various components at values suggested by Bloemen (1987), as well as the fractional composition of the components, and normalize the total midplane density of H I to give the measured column density. This midplane density is to be regarded here as a "mean" density, averaged over the projection of the line of sight onto the Galactic plane for the given direction. This simple model for the absorption appears to be adequate for our purposes. Even though a more detailed model of the structure of the local interstellar medium is necessary to accurately compute the diffuse flux at low energies (<0.3 keV), we justify our use of uniform absorption a posteriori by noting that (*i*) the stellar contribution at low energies to the diffuse background appears to be insignificant (see Table 3), and (*ii*) most of the stellar emission arises at distances greater than 100 pc,[5] and hence local variations in hydrogen column density may be ignored. Indeed, we expect large errors in the absorption model at the soft energy end of the passband considered here, but since the stellar flux contributions to the diffuse background are very low at these energies, these errors are unlikely to alter significantly our conclusions regarding stellar contributions to the diffuse flux at these energies. (The low values for the stellar flux contributions estimated for these energies seem invulnerable to the spatial and angular distribution uncertainties of the absorbing material, as long as we assume an "average" model for H I distribution. However, "leakage" of X-rays because of clumping and/or large-scale density fluctuations could alter this conclusion. We provide, for the sake of completeness, estimates of the stellar diffuse flux at these soft energies, subject to the caveat just stated.) For higher energies, the absorption effects are small, and hence the errors due to the absorption model would also be small. In contrast, the number counts of detected stars at very soft photon energies are strongly dependent on the absorption mechanism at low sensitivities. Hence, number count estimations at very soft energies are not reliable at low sensitivities. A detailed analysis of the stellar contribution to the diffuse flux at these very soft energies is in preparation (Kashyap 1992).

[5] In fact, assuming no absorption, the diffuse flux due to X-ray emission toward the direction $(l, b) = (0, 55)$ contributed by stars situated within 100 pc of the Sun, the distance within which most of the low energy diffuse background is believed to originate from a hot low density gas (see Snowden et al. 1990), is $\sim 7.6 \times 10^{-14}$ ergs s^{-1} cm^{-2} deg^{-2} in the C band. This is negligible compared to the total stellar diffuse flux in the same passband.

TABLE 3

COMPARISON OF THE STELLAR CONTRIBUTION TO THE DIFFUSE X-RAY BACKGROUND AS PREDICTED BY THE GALAXY MODEL AND THE OBSERVED BACKGROUND, AT TWO DIFFERENT LATITUDES

Passband	Observed Background	Galaxy Model ($b = 10$)/($b = 55$)	Percentages ($b = 10$)/($b = 55$)
[upper bound]		0.022/0.059	0.27/0.71
Be	8.4	0.015/0.041	0.19/0.50
[lower bound]		0.009/0.025	0.11/0.30
[upper bound]		0.42/1.06	1.1/1.5
B	38.5/72.5	0.31/0.78	0.8/1.1
[lower bound]		0.21/0.52	0.5/0.7
[upper bound]		2.93/5.42	3.1/2.9
C	95/184	2.13/3.94	2.2/2.1
[lower bound]		1.39/2.59	1.5/1.4
[upper bound]		2.74/1.51	16/7.8
M1	17.4/19.2	1.92/1.06	11/5.5
[lower bound]		1.18/0.65	6.8/3.4
[upper bound]		9.89/4.37	34/17
M2	28.9/25.9	6.84/3.02	24/12
[lower bound]		4.04/1.78	14/6.9
[upper bound]		34.7/13.2	71/30
I	49.0/43.4	23.9/9.09	49/21
[lower bound]		14.0/5.31	29/12
[upper bound]		45.9/15.4	66/22
J	69.1/68.2	31.6/10.6	46/15
[lower bound]		18.5/6.20	27/9.1
[upper bound]		0.06/0.14	0.56–1.35/1.31–3.13
L	4.6–11	0.05/0.11	0.42–1.00/0.96–2.30
[lower bound]		0.03/0.07	0.28–0.68/0.65–1.55
[upper bound]		1.90/1.05	20–41/11–23
M0	4.6–9.4	1.32/0.74	14–20/7.8–16
[lower bound]		0.79/0.45	8.4–17/4.8–9.7

NOTE.—The model predictions, and the corresponding upper and lower bounds due to the statistical 1 σ error on the mean luminosities, have been calculated. For the B, C, M1, M2, I, and J bands, the longitude averaged count rate at $b = 10$ and 55° (McCammon et al. 1983, McCammon 1991; see also McCammon & Sanders 1990) is compared with the galaxy model calculations for nominal directions of $(l, b) = (180, 10)$ and $(180, 55)$. The average Be band count rate (Bloch et al. 1986) is used for a similar comparison. The range of diffuse background flux (in units of 10^{-12} ergs s^{-1} cm^{-2} deg^{-2}) as estimated by Tanaka & Bleeker (1977) in the L band, and by Rosner et al. (1981) in the M0 band is also compared with model calculations (presented in the same units) for the same latitudes. A low instrument sensitivity was adopted in the stellar flux estimations, ensuring that all stars contribute to the diffuse background. Hydrogen column densities 2×10^{21} and 1.7×10^{20} cm^{-2} were used at $b = 10°$ and 55° respectively to account for absorption. It must be emphasized that the estimates at $b = 10°$ are subject to large uncertainties due to the patchiness of the absorption.

We calculate the absorption for a given value of the hydrogen column density in the following manner: The factor $e^{-\tau(r)}$ denoting the attenuation due to absorption in the interstellar medium in equations (8) and (10) is calculated at each distance step for both the quiet and active components of the emitted flux. To simplify the computations, this factor is actually interpolated from a two-dimensional grid calculated as a function of plasma temperature and column density in each band considered. For each temperature considered, the spectrum was attenuated by passing it through a column of interstellar matter quantified by a hydrogen column density, using an absorption cross section which is a piecewise polynomial fit

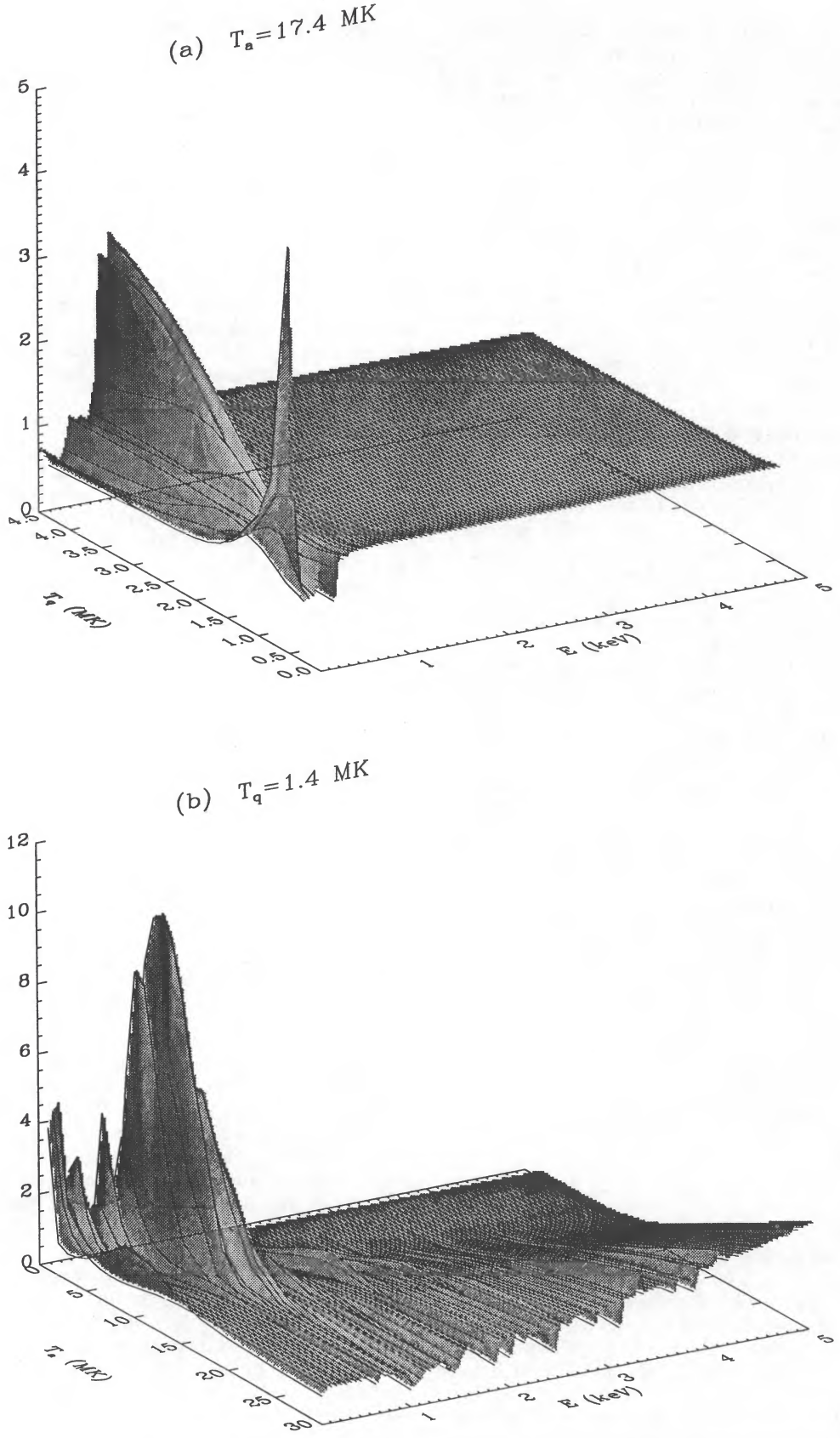

FIG. 2.—The variation of the stellar diffuse flux with energy in the 0.1–5 keV passband, with the variation in the temperatures assumed for the active and quiet components of the coronal emission model. The flux (averaged over 50 eV bins), normalized to the flux calculated adopting the best-fit values for the two temperature components, is calculated toward the north Galactic pole for a threshold sensitivity for point source detection $S \gg 10^{-10}$ ergs s^{-1} cm^{-2}, and a hydrogen column density of 2.1×10^{20} cm^{-2} as follows: (*a*) for various values of T_q, while fixing $T_a = 1.74 \times 10^7$ K, and (*b*) for various values of T_a, while fixing $T_q = 1.4 \times 10^6$ K.

to the interstellar photoelectric absorption cross section (Morrison & McCammon 1983), and the ratio of the attenuated to the unattenuated flux for each passband was stored. The optical depth is calculated at each distance and magnitude step by interpolating from these stored values.

3.6. *Temperature Variations (Two-Temperature Model)*

The effects of temperature variations on our calculations were explored simply by assuming different values for the active and quiet component temperatures. Conversion to bands other than the full *Einstein* band were then carried out as before. Optical depths were also calculated as before, taking the altered values of the temperatures into account.

We test for the sensitivity of estimates of stellar contributions to the diffuse background to variations in the temperatures assumed for the two components in two different ways: First, we consider stellar diffuse fluxes in narrow passbands at low sensitivities. These calculations may be compared with observations made by high-resolution spectrographs. Thus, we calculate the diffuse flux due to stellar emission in 50 eV bins at energies ranging from 0.1 to 5 keV for various values of the adopted temperatures, towards the north Galactic pole. We adopt a hydrogen column density of 2.1×10^{20} cm^{-2} in this direction. We find that generally, the computed fluxes are insensitive to small variations in the values adopted for the temperatures, and that variations in the temperature of the active region have a larger effect than variations in the temperature of the quiet region. Not surprisingly, the computed fluxes are most sensitive to the value of the adopted temperatures at the soft photon energy end of the pass band, where the flux is dominated by line emission. This can be seen in Figure 2, which plots the stellar diffuse flux (adopting a point source sensitivity of $S \gg 10^{-10}$ ergs s^{-1} cm^{-2}; all stellar sources contribute to the diffuse background) for various values of T_a (fixing $T_q = 1.4 \times 10^6$ K) and T_q (fixing $T_a = 1.74 \times 10^7$ K) normalized by the diffuse flux calculated for the temperatures adopted in the model (§ 3.2).

We also test for the effects of temperature variations on the stellar diffuse flux at higher sensitivities. For this purpose, we use broader bandpasses—the low-energy L band and the higher energy M band. We calculate log (f_{star})–log (S) curves in these passbands toward the north galactic pole, as above, for various values of the temperatures of the active and quiet components. The results are plotted in Figure 3. Once again, we find that the magnitude of the background flux is insensitive to small variations in the temperatures of the active and quiet component. In general, variations in the temperature of the active region has a larger effect than variations in the temperature of the quiet region. In all these cases, we hold the adopted spectrum for RS CVn stars to be invariant and note that at sensitivities $S < 10^{-14}$ ergs s^{-1} cm^{-2}, RS CVn stars do not contribute to the stellar diffuse flux at all as they become detections (see Fig. 8).

To test for the sensitivity of the number counts to temperature variations, we considered log (N)–log (S) curves calculated in the "broad" passband of 0.1–3.5 keV. Calculations performed in such broad bands are useful because at high sensitivities, number counts are generally available in only in broad bands. We find that log (N)–log (S) curves are to a high degree insensitive to temperature variations of both the quiet and the active components. This can be seen from the log (N)–log (S) curves for M(Blue) stars plotted in Figure 4, which are calculated toward the north Galactic pole for the same parameters as above.

3.7. *Model Variations*

We compare the two models assumed for the X-ray spectra (the two-temperature model and the power-law differential emission measure model) via the diffuse flux intensity spectrum due to stellar emission, calculated as outlined above. It is necessary to compare the flux intensity spectra and not the number counts, because as mentioned above, the number count determinations involve observations made in broad passbands, which reduce the sensitivity to spectral variations. Thus, we calculate the diffuse background flux intensity spectra due to stellar emission (averaged over 50 eV bins) for the energy range 0.1–5 keV for both spectral models. Both spectra were calculated toward the north Galactic pole for a hydrogen column density of $N_H = 2.1 \times 10^{20}$ cm^{-2}, for a very low point source detection threshold (so that we make sure that no stars were detected).

There are significant differences between the two approaches, the most striking being the prediction of maximum stellar contribution in the I band in the two-temperature case, and the M2 band in the exponential differential emission measure case (see Fig. 5). It must be pointed out that had Schmitt & Snowden (1990) used the maximum likelihood value for the mean luminosity of M dwarfs, they would have obtained a flux contribution ~ 3 times larger than they actually did in the M2 passband. Accounting for emission from other main-sequence stars would have lead to the conclusion that most of the M2 band flux results from stellar emission. Better determinations of emission measure distributions in stars, and a better understanding of the limitations of the application of the solar analogy, are required before the accuracy of the two models can be evaluated.

4. RESULTS

In this section, we describe the principal results of our calculations and our comparisons with available data.

4.1. *Diffuse X-Ray Flux Predictions for Specific Directions*

We have calculated the diffuse flux due to stellar emission for two "representative" directions: One at a high latitude of (l, b) = (180°, 55°) and another at a low latitude of (l, b) = (180°, 10°), assuming a low threshold sensitivity of point source detection, $S = 10^{-10}$ ergs s^{-1} cm^{-2} such that no stars are detected as sources. This facilitates comparisons with observed count rates and allows us to acquire an understanding of the importance of stellar emission in various passbands. The computed stellar diffuse fluxes were compared with the observed count rates and flux ranges reported by McCammon et al. (1983), Bloch et al. (1986), Tanaka & Bleeker (1977), and Rosner et al. (1981) in various bands (for bandwidth conventions used here, see Table 1).

A few remarks regarding our choice of directions is appropriate here. We consider predictions in two regions of the sky: at high latitudes ($|b| > 20°$), and low latitudes ($|b| < 20°$). To represent the high-latitude region, we chose the latitude 55°, not on the basis of any astronomical considerations, but rather because the stellar diffuse flux calculated for this latitude lies within the range of variation of the stellar diffuse flux that arises due to latitude variations (see below); that is, the stellar diffuse flux varies by a factor of 2 with variations in latitude at *high Galactic latitudes*, and much less due to variations in lon-

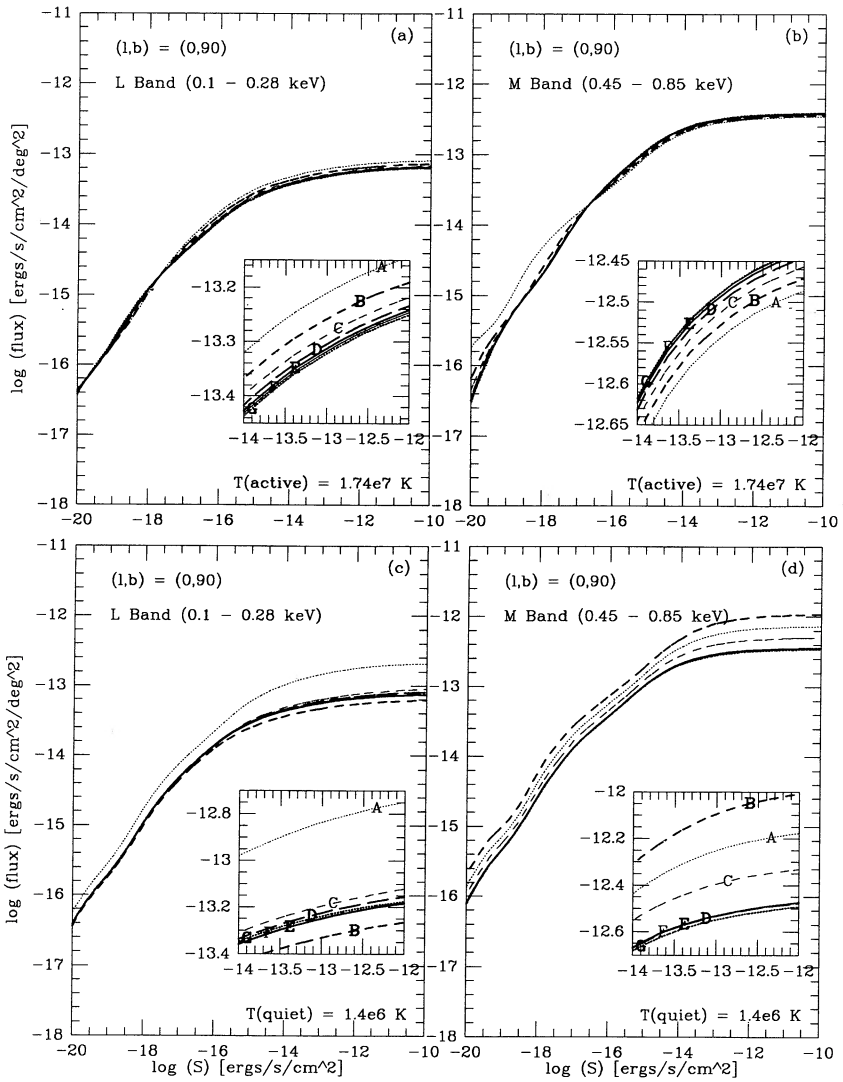

FIG. 3.—The variations of the stellar diffuse flux–sensitivity curves with the temperatures of the active and quiet regions. The abscissa represents the sensitivity of the instrument, S (ergs s^{-1} cm^{-2}); the ordinate is the background flux received at Earth due to stellar coronal emission, in units of ergs s^{-1} cm^{-2} deg^{-2}. The calculations have been performed for the direction toward the north Galactic pole, for a hydrogen column density $N_H = 2.1 \times 10^{20}$ cm^{-2}. (*a*) The temperature of the active region is held constant at 17.4×10^6 K, and the temperature of the quiet region is varied from 1 to 4×10^6 K (the labels A, B, C, D, E, F, and G correspond to 1, 1.5, 2, 2.5, 3, 3.5, and 4×10^6 K, respectively). The bandwidth considered is 0.1–0.28 keV (L band). (*b*) As (*a*), but in the 0.45–0.85 keV band (M band). (*c*) The temperature of the quiet region is held constant at 1.4×10^6 K, and the temperature of the active region is varied from 2 to 30×10^6 K (the labels A, B, C, D, E, F, and G correspond to 2, 6, 10, 14, 17, 20, and 30×10^6 K, respectively), for the same band as (*a*). (*d*) As (*c*), but in the 0.45–0.85 keV band (M band).

gitude and hydrogen column density, but both of these variations are less than the statistical variations associated with the high-luminosity tail of the luminosity functions (see below). The opposite is the case for low latitudes, where predictions are strongly dependent on longitude (as can be seen by comparing the stellar diffuse fluxes calculated for two different longitudes, but the same latitude, in Table 3 and Fig. 6), latitude (see Fig. 6), and the amount of hydrogen, both atomic and molecular, along the line of sight. Unfortunately, molecular hydrogen column densities vary widely, by nearly two orders of magnitude, and since at the high hydrogen column densities observed in the plane of the Galaxy, the optical depth of unity is reached at a few kpc, patchy absorption and excess molecular hydrogen can cause large departures from the flux predicted based on a smooth distribution of material. Therefore, to minimize such errors, we have adopted a latitude of 10° and a longitude of 180° to represent the stellar flux predictions at low latitudes.

The results of our calculations are tabulated in Table 3. For the total diffuse flux in the Be band, we have used the count rate averaged over eight fields as observed by Bloch et al. (1986); for the diffuse flux in the B, C, M1, M2, I, and J bands, we have used the longitude averaged count rate at latitudes $\sim 10°$ and 55° (McCammon 1991; McCammon et al. 1983); and for the L and M0 bands, we have adopted the range in flux as estimated by Tanaka & Bleeker (1977) and Rosner et al. (1981) respectively. At high Galactic latitudes, the stellar contribution to the diffuse flux in the low-energy bands (Be, B, C, and L) are very small (<3%), while the contributions in the higher energy bands (M1, M2, I, J, and M0) are significant, ranging from ≈3% to 30% depending on the passband. At low

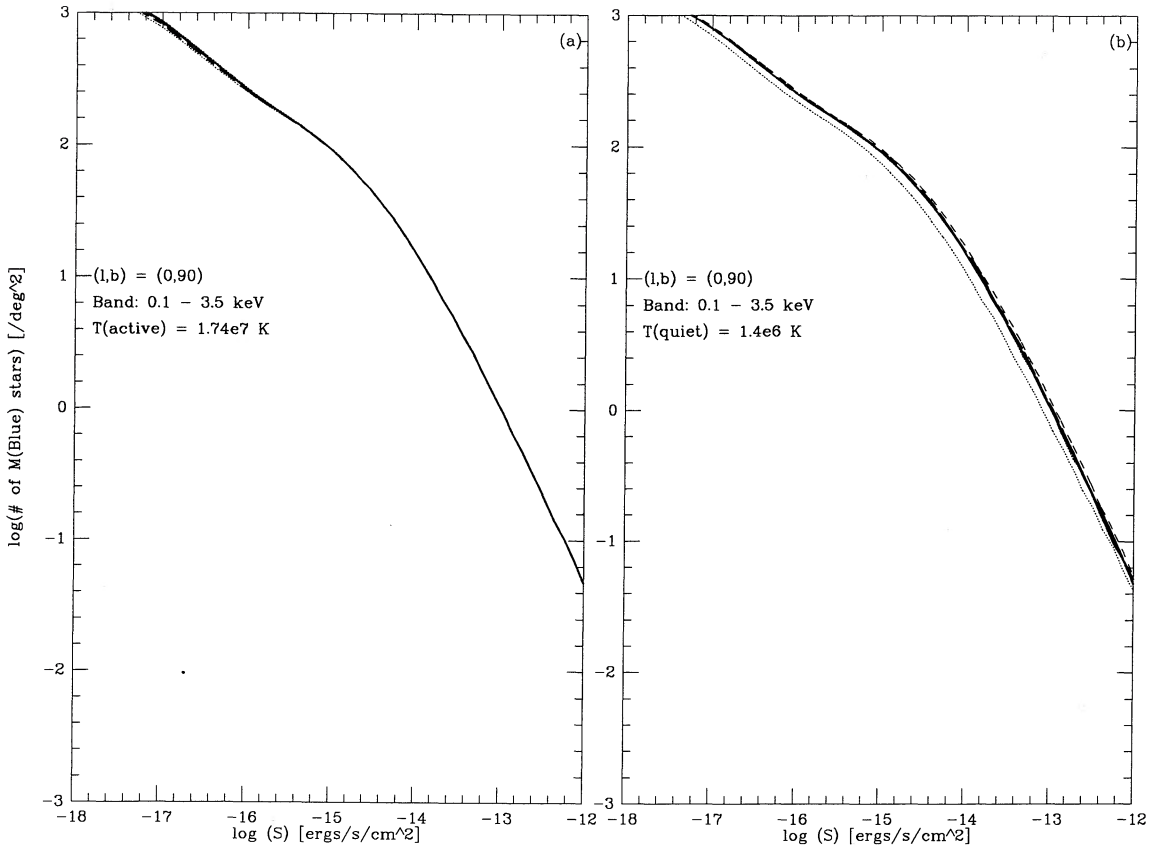

FIG. 4.—The variation of star counts with coronal temperature. We show the M(Blue) star log (N)–log (S) curves for a column density of 2.1×10^{20} cm^{-2} toward the north Galactic pole. The X-axis is the log of the sensitivity in units of ergs s^{-1} cm^{-2} deg^{-2}, and the Y-axis is the log of the number count. Note that these curves are essentially indistinguishable. (*a*) For quiet region temperatures from 1 to 4×10^6 K, for an active region temperature of 17.4×10^6 K. (*b*) For active region temperatures from 2 to 30×10^6 K, for a quiet region temperature of 1.4×10^6 K.

Galactic latitudes, the stellar contribution to the diffuse flux remains $<3\%$ in the low-energy bands, reflecting the high optical depths achieved in the plane of the Galaxy at these energies. However, in the higher energy bands, the stellar contribution increases drastically, varying from $\approx 7\%$ to 70%. As noted above, however, these figures are subject to large uncertainties and are given here only for the sake of completeness.

4.2. *Galactic Longitude and Latitude Variations of the Predicted Soft X-Ray Background*

We show the dependence of the diffuse stellar background on Galactic longitude and latitude in Figure 6. The diffuse flux in the M band, estimated for a latitude $b = 55°$, and adopting a low threshold sensitivity for point source detection ($S = 10^{-10}$ ergs s^{-1} cm^{-2}), is plotted for various longitudes in Figure 6*a*. The column densities are calculated using the three-component model of average gas distribution (eq. [12a]) in the Galaxy for $|b| > 20°$ and the empirical expression for the column density in the plane of the Galaxy (eq. [12b]) for $|b| \leq 20°$. The background fluxes calculated using measured H I column densities for the same directions are also plotted in Figure 6*a* for comparison. We note that variations in column density may be significant, but generally, such variations are much less than the statistical variations associated with the high-luminosity tail of the X-ray luminosity functions at high Galactic latitudes. Similarly, while there is a dependence of the background diffuse flux on longitude, this variation is also much less than the possible statistical fluctuations in the background at high Galactic latitudes (see discussion in § 4.1). The latitude dependence of the diffuse background due to stellar emission in the M, I, and J bands is shown in Figures 6*b*, 6*c*, and 6*d*, respectively. The calculations were performed for various values of Galactic latitudes and a nominal longitude of 90°. A low point source detection sensitivity of 10^{-10} ergs s^{-1} cm^{-2} was adopted. The results are plotted along with the observed longitude-averaged total diffuse flux in these bands (McCammon et al. 1983; McCammon 1991). As expected, the diffuse flux due to stellar emission drops with increasing latitude. In none of the bands does the latitude dependence of the stellar emission match that of the total diffuse background, even though at high energies (I and J bands), stellar emission forms a major fraction of the total background.

4.3. *Fractional Contributions to the Diffuse Soft X-Ray Background*

The fractional flux contribution of each spectral type to the stellar diffuse flux, as calculated adopting the two-temperature model for the emission of X-rays from stars is tabulated in Table 4A. These values are sensitive to energy only over the range of energies where interstellar absorption is a major factor in the determination of the stellar contribution to the diffuse flux. This is not surprising, since we use a two-

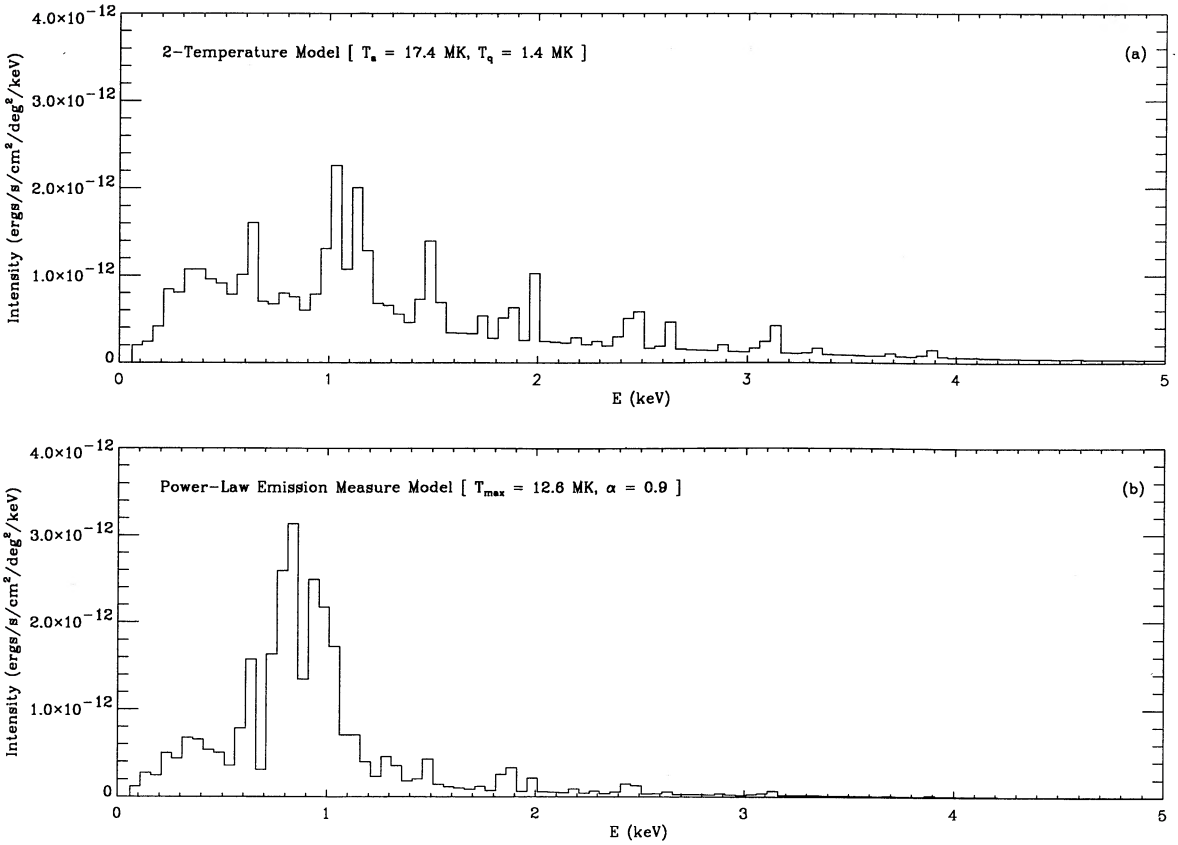

FIG. 5.—The intensity of the stellar diffuse emission. The diffuse stellar background emission, in units of ergs s^{-1} cm^{-2} keV^{-1}, calculated toward the north Galactic pole, is plotted for energies ranging from 0.1 to 5 keV. The point source detection threshold is set at a very low value so as to maximize the stellar contribution. (*a*) The intensity spectrum as calculated for the two-temperature coronal emission model. (*b*) The spectrum calculated assuming a power-law emission measure model for stellar coronal emission.

component spectrum that is not altered except by absorption, and hence the fractions of each spectral type contributing to the stellar diffuse emission remains nearly constant where stellar contribution to the diffuse background is significant. It is seen that early-type M stars are the major contributor to the diffuse stellar flux. However, neglecting the contributions from stars of other spectral types leads to underestimates of the diffuse stellar flux, ranging from ~40% for I and higher energy bands to ~45% for the softer M1 and M2 bands.

For comparison, we performed the same calculations adopting the power-law emission measure model to describe the emission of X-rays from stars. The results are tabulated in Table 4B. Once again, we see that early-type M stars contribute about 50% of the stellar flux at low energies, 57% at medium energies, and about 45% at higher energies. In this model, RS CVn stars begin to contribute more to the stellar diffuse flux at higher energies, as expected from the harder spectrum adopted for it (see § 3.2).

4.4. *The Effects of Improved Point Source Detection Thresholds*

The effect of improved instrument sensitivity on the magnitude of the background flux is considered in the case of the M, E, and R bands, and the results are tabulated in Table 5. Improved sensitivity has little effect on the background flux for sensitivities as high as 10^{-14} ergs s^{-1} cm^{-2} because most of the contributing stars emit below this flux level. However, there is a significant dependence on point source sensitivity in terms of the number of stars detected as X-ray emitters. While the *Einstein Observatory*, with a typical sensitivity of $\sim 10^{-13}$ ergs s^{-1} cm^{-2}, was capable of detecting about two stars per square degree toward the north Galactic pole in the 0.1–3.5 keV band, the *AXAF* (*Advanced X-ray Astronomy Facility*), to be launched by NASA in the late 1990s, with a typical sensitivity of $\sim 10^{-15}$ ergs s^{-1} cm^{-2}, would detect ~175 stars per square degree [seven F, 11 G, 26 K, 91 M(Blue), and 40 M(Red) stars] in this band in the same direction.

The dependence of the background flux on the threshold sensitivity for point source detection can be seen in greater detail in Figure 7. Background fluxes for sensitivities ranging from 10^{-10} to 10^{-20} ergs s^{-1} cm^{-2} for two bands (the L and M bands) were calculated towards the north Galactic pole, using a hydrogen column density of 2.1×10^{20} cm^{-2}. As expected, the background flux changes little for low sensitivities, drops at threshold sensitivities where most disk stars are detected, and drops again when most spheroid stars are detected. For sensitivities as high as 10^{-14} ergs s^{-1} cm^{-2}, however, the diffuse flux due to stellar emission is more than $\frac{2}{3}$ of the total stellar flux at Earth.

The sensitivity range over which the background flux drops sharply depends not only on the band and the direction of observation, but also weakly on the temperature of the active regions of the emitter; in contrast, this range is insensitive to

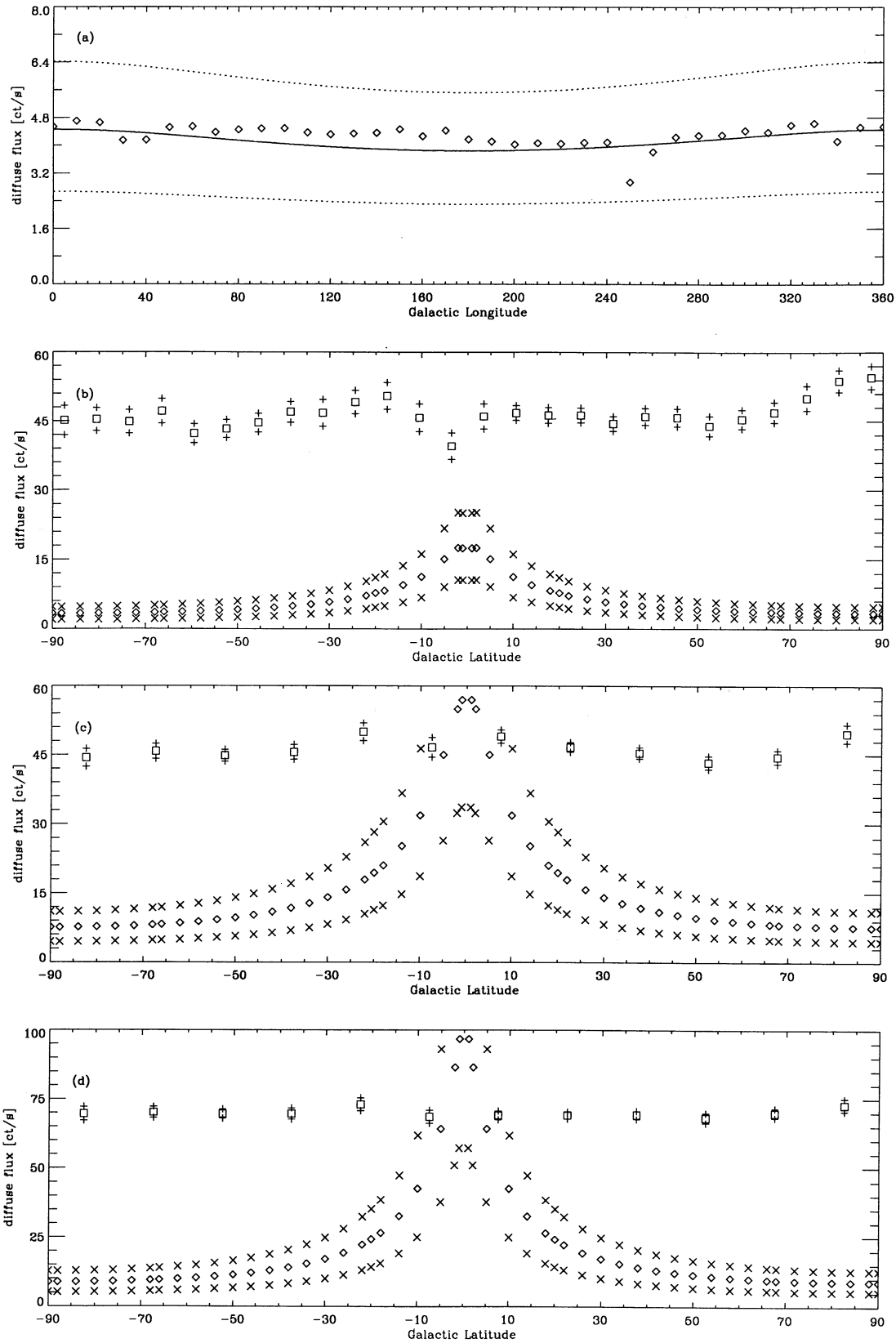

FIG. 6.—The longitude and latitude dependence of the stellar contribution to the diffuse X-ray background. The ordinate is the diffuse X-ray count rate in each of the mentioned passband as determined from McCammon et al. (1983; also McCammon 1991), with the stellar diffuse flux calculated for a point source detection sensitivity of 10^{-10} ergs s^{-1} cm^{-2}. (*a*) The stellar diffuse flux calculated for a latitude of 55° and various longitudes. The solid line is the flux calculated by adopting the model for the average gas distribution in the Galaxy (Bloemen 1987); the dotted lines represent the upper and lower bounds on the computed fluxes due to the 68% confidence limits on the mean luminosities. The diamonds represent the flux as calculated using measured column densities (Heiles & Habing 1974) for the same directions (see § 3.5). (*b*) The contribution of all types of stars to the diffuse X-ray background in the M band, calculated for a longitude of 90°, and various latitudes. The diamonds represent the calculated stellar fluxes; the crosses represent the upper and lower bounds on them due to 68% confidence limits on the mean luminosities that arise due to statistical fluctuations in the high-luminosity tail of the luminosity functions. The observed total diffuse background flux averaged over longitude (McCammon et al. 1983) is also plotted as square boxes, including the appropriate 1 σ errors (*plus signs*). (*c*) As (*a*), but in the I band. (*d*) As (*a*), but in the J band.

TABLE 4

PERCENTAGE CONTRIBUTION BY STELLAR TYPE TO THE STELLAR DIFFUSE FLUX AT VARIOUS ENERGIES

E(keV)	A	F	G	K	M(Blue)	M(Red)	RS CVn
A. Two-Temperature Model[a]							
0.15.....	0.58	6.67	5.07	11.8	49.2	15.1	11.6
0.25.....	0.50	6.16	6.17	13.4	48.3	17.1	8.29
0.50.....	0.12	4.26	4.57	12.2	56.9	15.5	6.40
0.75.....	0.01	3.99	4.30	11.7	56.1	14.9	8.81
1.0.....	0.09	4.04	4.37	12.1	58.4	15.4	5.63
1.5.....	0.09	4.08	4.42	12.2	59.2	15.6	4.45
2.0.....	0.09	4.09	4.43	12.3	59.4	15.6	4.14
3.0.....	0.09	4.11	4.46	12.3	59.7	15.7	3.67
B. Power-Law Emission Measure Model							
0.15.....	0.36	6.62	4.79	11.6	51.4	15.0	10.2
0.25.....	0.18	4.87	4.56	11.3	50.4	14.7	13.9
0.50.....	0.14	4.49	4.68	11.8	52.2	15.2	11.5
0.75.....	0.15	4.85	5.09	12.8	56.9	16.6	3.63
1.0.....	0.15	4.84	5.10	12.8	57.0	16.6	3.40
1.5.....	0.13	4.27	4.52	11.4	50.5	14.7	14.4
2.0.....	0.12	4.00	4.23	10.6	47.3	13.8	19.9
3.0.....	0.11	3.83	4.05	10.2	45.3	13.2	23.2

NOTE.—The stellar fluxes were calculated in 50 eV bins toward the north Galactic pole, adopting a hydrogen column density of $N_H = 2.1 \times 10^{20}$ cm^{-2}, and assuming that the detection sensitivity threshold is low enough that all stars contribute to the diffuse background.

[a] Stellar diffuse fluxes calculated adopting the two-component model of stellar X-ray emission as described in § 3.2.

[b] Stellar diffuse flux calculated adopting the power-law emission measure model of stellar X-ray emission as described in § 3.2.

TABLE 5

THE STELLAR CONTRIBUTION TO THE SOFT X-RAY BACKGROUND AS A FUNCTION OF THE SENSITIVITY OF THE DETECTOR

SENSITIVITY (ergs s^{-1} cm^{-2})	BACKGROUND FLUX × 10^{13} (ergs s^{-1} cm^{-2} deg^{-2}) E[a]	M[b]	R[c]
⟨95% upper limit⟩	65.1	10.5	70.7
10^{-10}	24.9	4.52	27.5
⟨95% lower limit⟩	14.2	2.61	15.7
⟨95% upper limit⟩	41.3	8.93	45.7
10^{-12}	22.0	4.28	24.3
⟨95% lower limit⟩	11.8	2.42	13.0
⟨95% upper limit⟩	32.6	6.40	35.5
10^{-13}	18.1	3.87	19.8
⟨95% lower limit⟩	9.91	2.15	10.8
⟨95% upper limit⟩	17.3	4.61	18.2
10^{-14}	11.3	3.02	12.1
⟨95% lower limit⟩	7.05	1.72	7.52
⟨95% upper limit⟩	6.82	2.35	7.27
10^{-15}	4.73	1.70	5.01
⟨95% lower limit⟩	3.35	1.03	3.56
⟨95% upper limit⟩	3.32	1.01	3.61
10^{-16}	1.96	0.69	2.09
⟨95% lower limit⟩	1.34	0.51	1.42

NOTE.—Calculations are carried out for the *Einstein* (E), M, and *ROSAT* (R) bands along the direction (l, b) = (0, 55) for a hydrogen column density of 3.66×10^{20} cm^{-2}.

[a] Multiplying the numbers in this column by 4×10^{-3} gives the approximate count rate in the *Einstein* IPC in units of counts s^{-1} deg^{-2}. This energy to count rate conversion factor varies with N_H and S, but this variation is much less than the statistical uncertainties in the calculations.

[b] Multiplying the numbers in this column by 1.002 gives the approximate count rate in the M band of the Wisconsin All-Sky Survey (McCammon et al. 1983) in units of counts s^{-1}.

[c] Multiplying the numbers in this column by 2.8×10^{-6} gives the approximate count rate in the *ROSAT* PSPC in units of counts s^{-1} arcmin^{-2}.

variations in quiet region temperatures (see § 3.6). This can be seen from Figure 3, which plots the background fluxes calculated for various combinations of the temperatures for the same direction and bands as in Figure 7.

4.5. *Number Count Predictions*

The log (N)–log (S) curves for all stars, and for each spectral type considered [A, F, G, K, M(Blue), M(Red), and RS CVn], calculated for the 0.1–3.5 keV band, and the 68%, 95%, and 99% confidence limits on them are presented in Figure 8. The curves were calculated adopting a column density of 2.1×10^{20} cm^{-2} toward the north Galactic pole. Contributions from the spheroid component of the galaxy model are insignificant for sensitivities $S > 10^{-16}$ ergs s^{-1} cm^{-2}.

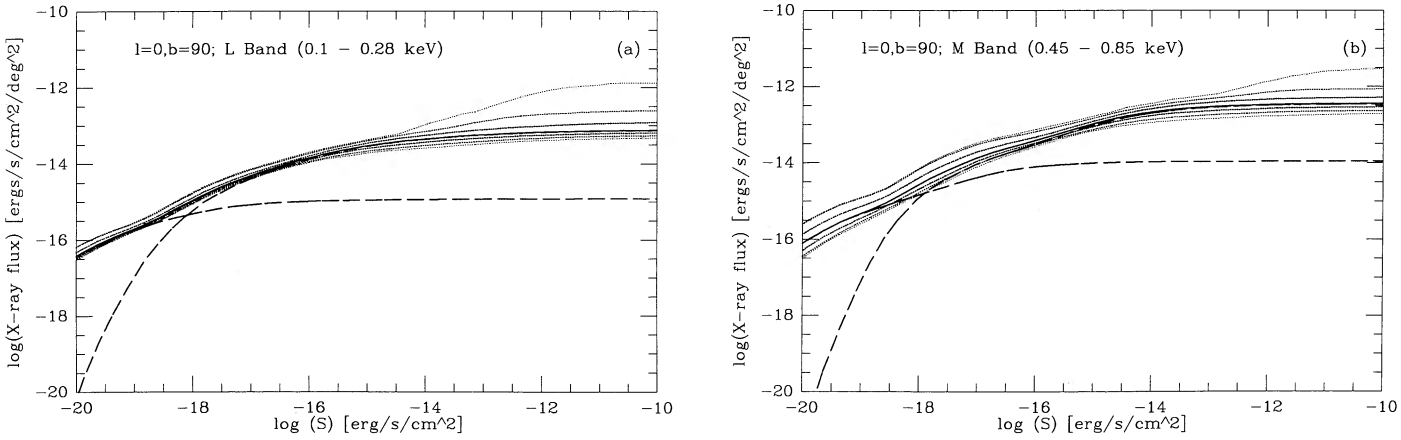

FIG. 7.—The variation of the stellar diffuse flux with point source detection sensitivity threshold. The abscissa represents the sensitivity of the instrument, S (ergs s^{-1} cm^{-2}), and the ordinate is the diffuse stellar flux received at Earth, in units of ergs s^{-1} cm^{-2} deg^{-2}. The dashed lines are the contributions from the disk and the spheroid components. The calculations have been performed toward the north Galactic pole, for a hydrogen column density $N_H = 2.1 \times 10^{20}$ cm^{-2}. Note that the diffuse flux does not decrease by more than ~33% for sensitivities as high as 10^{-14} ergs s^{-1} cm^{-2}. (*a*) Fluxes in the L band. (*b*) Fluxes in the M band.

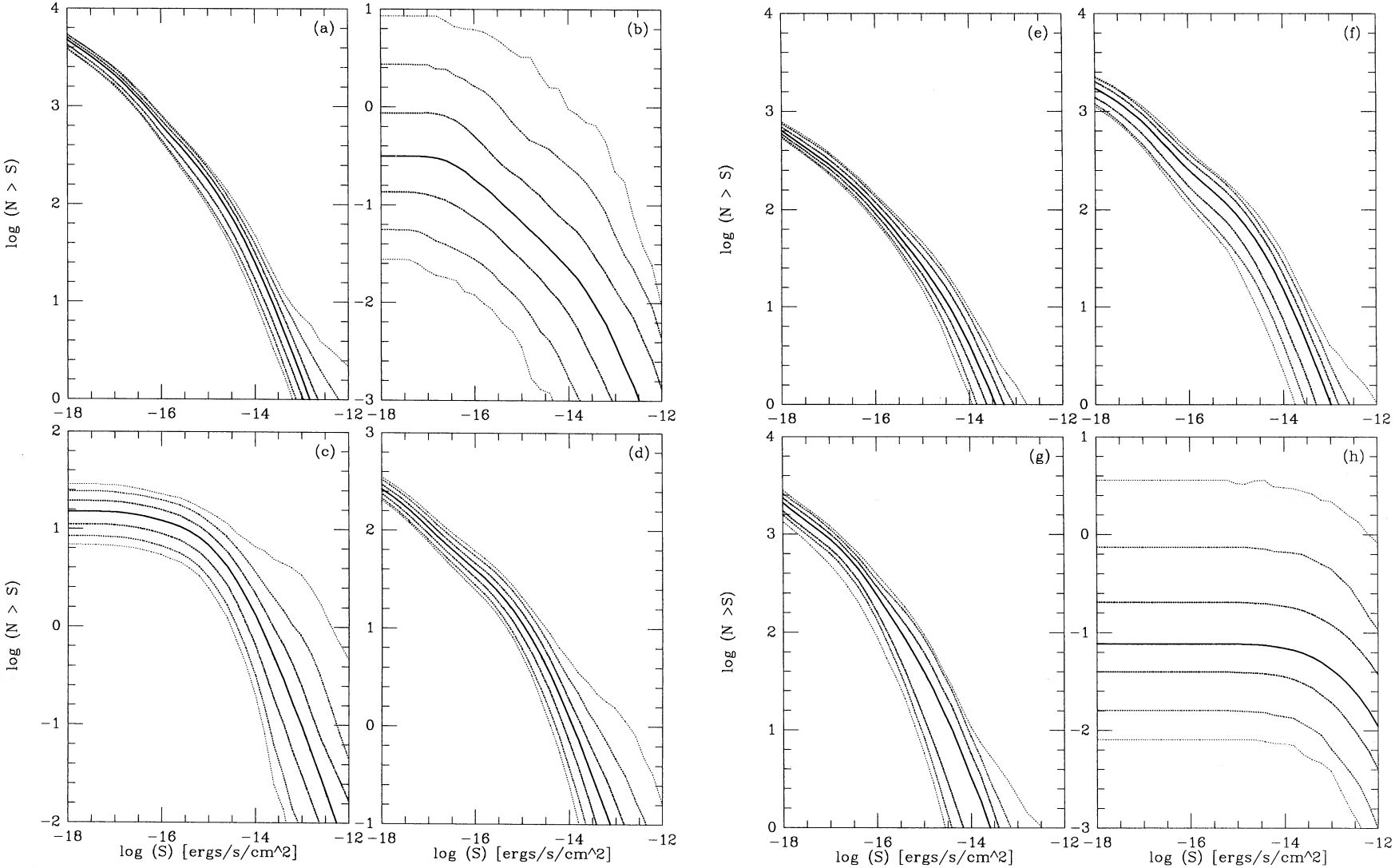

FIG. 8.—The log (N)–log (S) curves for main-sequence stars; in each case, the abscissa represents the X-ray sensitivity level S (ergs s^{-1} cm^{-2}), while the ordinate represents the number of stars per square degree detected at sensitivity levels greater than or equal to S. The solid line is the curve predicted by the galaxy model; the dotted lines are the corresponding 68%, 95%, and 99% confidence limits. The calculations were performed toward the north Galactic pole. A hydrogen column density $N_H = 2.1 \times 10^{21}$ cm^{-2} has been used. (*a*) The log N–log S curve for all stars. (*b*) As (*a*), but for A stars. (*c*) As (*a*), but for F stars. (*d*) As (*a*), but for G stars. (*e*) As (*a*), but for K stars. (*f*) As (*a*), but for M(Blue) stars. (*g*) As (*a*), but for M(Red) stars. (*h*) As (*a*), but for RS CVn stars.

4.6. *Comparison of Predicted and Observed Stellar Number Counts*

The star counts predicted by the galaxy model for a representative direction of $(l, b) = (0°, 55°)$ using a hydrogen column density of 3.66×10^{20} cm^{-2} are compared with the counts predicted by Favata et al. (1988) and the observed counts in the Medium Sensitivity Survey (MSS), the High Sensitivity Survey (HSS), and the Hyades Region Survey (HRS) in Table 6. The bandwidths and sky coverage of these surveys as well as the 95% confidence limits on the calculated counts (obtained as outlined in § 3) are also given in Table 6. For a more detailed discussion of these surveys, see Favata et al. (1988).

In the MSS, the sensitivity varies over nearly two orders of magnitude, so that the numbers calculated here for the sensitivities mentioned are nominal; the calculated numbers indicate that it is not impossible to obtain the observed number counts. In the HSS, the observed counts are well within the 95% confidence limit of the predicted counts for all types except for A and F spectral types. In the HRS too, the predicted counts are in good agreement with the observed numbers, even though the best-fit predicted counts for G stars is low.

The discrepancy in the RS CVn star counts calculated here, using the simple exponential distribution model with the parameters for RS CVn stars listed in Table 2, and those calculated by Favata et al. (1988), is undoubtedly due to the difference in the luminosity functions used.

TABLE 6

STAR COUNTS PREDICTED BY GALAXY MODEL

Sensitivity (ergs s^{-1} cm^{-2})	A	F	G	K	M(Blue)	M(Red)	RS CVn
A. MSS (Medium Sensitivity Survey): Bandwidth, 0.3–3.5 keV; area covered, 90 deg^2. Sensitivities vary from 7.1×10^{-14} to 2.0×10^{-12} ergs s^{-1} cm^{-2}							
[+95% level]	8.7	97.1	50.9	119.1	473.1	115.4	68.54
7.08×10^{-14}	0.51	13.9	9.5	42.7	164.6	22.2	7.4
[−95% level]	0.01	1.2	1.1	8.1	23.3	0.6	1.2
[+95% level]	1.4	13.9	7.8	24.7	66.7	21.8	28.0
3.98×10^{-13}	0.07	1.4	0.9	4.3	15.4	2.0	2.9
[−95% level]	0.001	0.12	0.09	0.36	0.8	0.08	0.28
[+95% level]	0.4	3.3	1.1	10.5	29.0	8.1	13.3
1.00×10^{-12}	0.02	0.4	0.23	1.1	4.1	0.54	1.4
[−95% level]	0.0	0.03	0.02	0.1	0.2	0.02	0.11
[+95% level]	0.13	1.2	0.7	4.4	14.9	3.3	7.1
2.00×10^{-12}	0.008	0.14	0.09	0.4	1.5	0.2	0.7
[−95% level]	0.0	0.01	0.008	0.04	0.09	0.006	0.06
Favata et al.	1.3		1.2	3.8	10.0		3.1
Observed	5		9	10	6		...
B. HSS (High Sensitivity Survey): Bandwidth, 0.8–3.5 keV; area covered, 1.5 deg^2 at 5.5×10^{-14} ergs s^{-1} cm^{-2} and 0.8 deg^2 at 3.98×10^{-14} ergs s^{-1} cm^{-2}							
[+95% level]	0.08	1.0	0.6	1.4	5.3	1.1	0.7
3.98×10^{-14}	0.006	0.18	0.13	0.6	2.1	0.29	0.08
[−95% level]	0.0	0.01	0.02	0.13	0.3	0.008	0.01
[+95% level]	0.1	1.5	0.87	2.1	7.0	1.5	1.2
5.5×10^{-14}	0.008	0.2	0.16	0.7	2.7	0.36	0.1
[−95% level]	0.0	0.016	0.019	0.1	0.38	0.01	0.02
[+95% level]	0.2	2.5	1.5	3.5	12.4	2.7	2.0
Total	0.01	0.4	0.3	1.3	4.9	0.66	0.2
[−95% level]	0.0	0.03	0.04	0.25	0.7	0.02	0.03
Favata et al.	0.3		0.3	1.0	2.5		1.1
Observed[a]	3		1	0	2 + (2)		...
C. HRS (Hyades Region Survey): Bandwidth, 0.2–4.0 keV; area covered, 16.5 deg^2 at a typical sensitivity 1.38×10^{-13} ergs s^{-1} cm^{-2}							
[+95% level]	0.7	10.8	5.2	12.1	34.3	9.0	10.0
1.38×10^{-13}	0.05	1.17	0.77	3.5	12.7	1.8	1.1
[−95% level]	0.0	0.09	0.08	0.5	1.2	0.07	0.15
Favata et al.	0.9		0.9	2.7	7.0		1.8
Observed	2		6	2	7		...

NOTE.—Comparison of the star counts predicted by the galaxy model for a nominal direction of $(l, b) = (0, 55)$ with their 95% upper and lower confidence limits, and Favata et al. (1988) in the MSS, HSS, and the HRS with the observed counts. A hydrogen column density $N_H = 3.66 \times 10^{20}$ cm^{-2} was used towards this nominal direction. It must be noted that variations of as much as a factor of two can be introduced by latitude and longitude variations, and hence are not significant.

[a] Two stars without known optical counterparts have been included in the entry for M stars within parentheses (Favata et al. 1988).

5. SUMMARY

Using the X-ray luminosity functions for A, F, G, K, M(Blue), M(Red), and RS CVn stars and star counts generated by the galaxy model of Bahcall & Soneira (1980), log $(N > S)$–log (S) curves have been constructed. Star counts expected for the *Einstein* surveys were calculated using these curves and were compared with the observed stellar counts compiled by Favata et al. (1988). The observed star counts are generally—but not always—within the 68% confidence limit of the number predicted by our X-ray galaxy model. In particular, the A and F star counts are within 68% limits for the Medium Sensitivity Survey (MSS) and the Hyades Region Survey (HRS), but not the High Sensitivity Survey (HSS); the G star counts are within the 68% limits for the MSS, but not the HSS and the HRS. Finally, our predicted RS CVn star counts are less than those predicted by Favata et al. (1988) on the basis of a very simple galaxy model; there is insufficient observational data available at present to judge whether our predictions are borne out by the observations.

The diffuse soft X-ray background flux due to stars drops by $\sim 50\%$ as the sensitivity of the detecting instruments is increased to 10^{-14} ergs s^{-1} cm^{-2}. The number of detected stars increases with an average power 1.3 of the sensitivity in this sensitivity range; more specifically, the slope of the log (N)–log (S) curve varies locally from ≈ -1.4 near $S = 10^{-10}$ ergs s^{-1} cm^{-2} to ≈ -1.1 near $S = 10^{-14}$ ergs s^{-1} cm^{-2}. Thus, even at a point source sensitivity of 10^{-14} ergs s^{-1} cm^{-2}, it appears that one will not be detecting most of the stars which contribute to the diffuse background. About 80% of the stellar diffuse emission comes from stars that would be detected at a point source sensitivity of $\sim 10^{-15}$ ergs s^{-1} cm^{-2} (this figure depends very sensitively on latitude and hydrogen column density and can decrease to 10^{-17} for low latitudes), which constitutes a very small fraction of the total number of X-ray–emitting stars in the specified direction.

The diffuse background fluxes as calculated by Rosner et al. (1981) are within the 68% confidence limit of the diffuse background fluxes calculated here (for an instrument sensitivity of 10^{-10} ergs s^{-1} cm^{-2}); we believe that whatever differences there are can be attributed to our use of more sophisticated models for the Galactic stellar spatial distribution and ISM absorption characteristics and better estimates of the stellar X-ray luminosity functions. By comparing the fluxes calculated using our galaxy model with the observed fluxes (e.g., McCammon et al. 1983), we thus confirm the conclusions of Rosner et al. (1981) that stars contribute significantly to the diffuse X-ray background in the 0.3–2 keV energy band.

Our results also show that background observations with high-energy resolution may potentially shed much light on the nature of the sources contributing to the sources. Unlike the case of broad-band observations, data with energy resolution of as little as 50 eV show substantial sensitivity to the nature of the background sources, viz., the temperature of the active stellar component.

A major limitation of our results is our resort to mean models for the Galactic stellar and gas distributions: Our comparison of results based on the Heiles & Habing (1974) and Bloemen (1987) Galactic hydrogen distribution determinations suggest that there may be very large local disparities from the mean descriptions given here. This effect is enormously pronounced at softer photon energies (e.g., <0.5 keV), and near the Galactic plane ($|b| < 20°$), and will be accentuated if observations are carried out at high-energy resolution.

We would like to thank Priscilla Frisch for comments and for help in determining the hydrogen column densities. We also wish to thank the referee, Dan McCammon, for very useful comments regarding both the substance and the layout of this paper. This research has benefited from the use of software and/or datasets assembled for the Local Interstellar Matter Workshop project at the University of Chicago. Financial support for the Workshop has been provided by NASA grants NAG5-704, NAG5-1303, and NAG5-286 to the University of Chicago. This work was supported in part by NASA grants to the University of Chicago and the Smithsonian Astrophysical Observatory, and by grants from Ministero Universitá Ricerca Scientifica e Tecnologica and from Agenzia Spaziale Italiana to the Osservatorio Astronomico di Palermo.

REFERENCES

Allen, C. W. 1973, Astrophysical Quantities (London: Athlone)
Bahcall, J. N. 1986, private communication
Bahcall, J. N., & Soneira, R. M. 1980, ApJS, 44, 73
Bloemen, J. B. G. M. 1987, ApJ, 322, 694
Bloch, J. J., Jahoda, K., Juda, M., McCammon, D., Sanders, W. T., & Snowden, S. L. 1986, ApJ, 308, L59
Bookbinder, J. 1987, Ph.D. thesis, Harvard University
Burrows, D. N., McCammon, D., Sanders, W. T., & Kraushaar, W. L. 1981, BAAS, 13, 882
Caillault, J.-P. 1990, PASP, 102, 989
Caillault, J.-P., Helfand, D. J., Nousek, J. A., & Takalo, L. O. 1986, ApJ, 304, 318
Cruddace, R., Paresce, F., Bowyer, S., & Lampton, M. 1974, ApJ, 187, 497
Davidsen, A., Shulman, S., Fritz, G., Meekins, J. F., Henry, R. C., & Friedman, H. 1972, ApJ, 177, 629
Dickey, J. M., & Lockman, F. J. 1989, ARA&A, 28, 215
Favata, F. 1987, Laurea thesis, University of Palermo
Favata, F., Rosner, R., Sciortino, S., & Vaiana, G. S. 1988, ApJ, 324, 1010
Feigelson, E. D., & Nelson, P. I. 1985, ApJ, 293, 192
Fried, P. M., Nousek, J. A., Sanders, W. T., & Kraushaar, W. L. 1980, ApJ, 242, 987
Gorenstein, P., & Tucker, W. H. 1972, ApJ, 176, 333
Hall, D. S. 1976, in Multiple Periodic Variable Stars, ed. W. S. Fitch (Dordrecht: Reidel), 287
Heiles, C., & Habing, H. J. 1974, A&AS, 14, 1
Kashyap, V. 1992, in preparation
Levine, A., Rappaport, S., Halpern, J., & Walter, F. 1977, ApJ, 211, 215
Long, K. S., Agrawal, P. C., & Garmire, G. P. 1976, ApJ, 206, 411
Luyten, W. J. 1968, MNRAS, 139, 22
Maggio, A., et al. 1987, ApJ, 315, 687
Majer, P., Schmitt, J. H. M. M., Golub, L., Harnden, F. R., Jr., & Rosner, R. 1986, ApJ, 300, 360
McCammon, D. 1991, private communication
McCammon, D., Bunner, A. N., Coleman, P. L., & Kraushaar, W. L. 1971, ApJ (Letters), 168, L33
McCammon, D., Burrows, D. N., Sanders, W. T., & Kraushaar, W. L. 1983, ApJ, 269, 107
McCammon, D., Meyer, S. S., Sanders, W. T., & Williamson, F. O. 1976, ApJ, 209, 46
McCammon, D., & Sanders, W. T. 1990, ARA&A, 28, 657
Micela, G., Harnden, F. R., Jr., Rosner, R., Sciortino, S., & Vaiana, G. S. 1991, ApJ, 380, 495
Morrison, R., & McCammon, D. 1983, ApJ, 270, 119
Press, W. H., Flannery, B. P., Teukolsky, S. A., & Vetterling, W. T. 1986, Numerical Recipes (Cambridge: Cambridge Univ. Press)
Raymond, J. C. 1986, private communication
Raymond, J. C., & Smith, B. W. 1977, ApJS, 35, 419
Rosner, R., et al. 1981, ApJ, 249, L5
Rosner, R., Golub, L., & Vaiana, G. S. 1985, ARA&A, 23, 413
Schmitt, J. H. M. M. 1985, ApJ, 293, 178
Schmitt, J. H. M. M., Collura, A., Sciortino, S., Vaiana, G. S., Harnden, F. R., Jr., & Rosner, R. 1990, ApJ, 365, 704
Schmitt, J. H. M. M., Golub, L., Harnden, F. R., Jr., Maxson, C. W., Rosner, R., & Vaiana, G. S. 1985, ApJ, 290, 307
Schmitt, J. H. M. M., & Snowden, S. L. 1990, ApJ, 361, 207
Schwartz, D. A., & Gursky, H. 1973, in Gamma-Ray Astrophysics, ed. F. W. Stecker & J. I. Trombka (NASA-SP-339), 15
Snowden, S. L., Cox, D. P., McCammon, D., & Sanders, W. T. 1990, ApJ, 354, 211
Tanaka, Y., & Bleeker, J. A. M. 1977, Space Sci. Rev., 20, 815
Vanderhill, M. L., Borken, R. J., Bunner, A. N., Burstein, P. H., & Kraushaar, W. L. 1975, ApJ, 197, L19
Vaiana, G. S., & Rosner, R. 1978, ARA&A, 26, 393
Wielen, R. 1974, Highlights Astron., vol. 3, 395